human hematopoietic cells present in the diaphyseal shaft were counted under light microscopy with assistance of a Zeiss KS400.

Interaction between human MSCs and human HSCs. Entire fields of longitudinal sections cut through the center of bones were examined for cell counting. All eGFP-expressing cells and immunophenotyped human hematopoietic cells present in BM were counted under fluorescent microscopy. When cells were in physical contact, they were categorized as interacting.

Statistical analysis

All values are presented as the mean plus or minus standard deviation (SD). The 2-sided *P* value was determined, testing the null hypothesis that the 2 population medians are equal. *P* below .05 was considered significant.

Results

Spatial distribution of human hematopoietic cells in the murine BM compartment

The potential of human HSCs in vivo can be assessed by using the SCID-repopulating cell (SRC) assay based on the ability to reconstitute hematopoiesis in the host following transplantation into NOD/SCID mice.[20] However, analysis of SRCs by flow cytometry does not allow identification of individual SRCs in situ. Consequently, the behavior of transplanted SRCs during repopulation has not been elucidated. To address this issue, we prepared mice that were highly chimeric with human hematopoietic cells by directly injecting CBCD34 cells into the tibia[12] and investigated the spatial organization of individual engrafted cells in murine BM at 10 weeks after transplantation. Close examination of the bone specimens revealed that cells stained positive for human CD34, a marker of human HSCs and progenitor cells, were specifically localized to an area near the endosteum of the bone (the endosteal region) (Figure 1A). In contrast, cells positively stained for human CD15, a marker of committed myelocytes, or glycophorin A (GlyA), a marker of the erythrocyte lineage, were distributed distant to the endosteum (Figure 1B-C). These results reflect previous morphologic studies of BM that found that hematopoietic stem and progenitor cells are concentrated in the endosteal region rather than the central marrow area, which mostly is composed of mature cells.[19,21,22] To quantitatively confirm these observations, the numbers of $CD34^+$, $CD15^+$, and $GlyA^+$ cells present in the endosteal region or in the central BM cavity of the diaphyseal shaft were counted. Consistent with the microscopic observations, a surprisingly higher proportion of $CD34^+$ cells was located in the endosteal region compared to the lineage-committed cells (Table 1). Because the endosteal region consisted of only 21.4% ± 3.8% of the BM cavity examined for this assay, there were approximately 10-fold more $CD34^+$ cells in the endosteal area. By visualizing the fate of transplanted SRCs in situ and confirming their physiologic organization in BM, these results validate the SRC assay for human cell analysis. Hence, we used this xenogeneic transplantation system for the phenotypic and functional characterization of human MSCs in vivo.

Visualization of human MSCs and human CBCD34 engraftment in the murine BM compartment

The route of administration is an important factor for effective delivery of transplanted cells into the target tissue. We compared the degree of cell engraftment in BM at 4 and 10 weeks after IBMT or intravenous transplantation of eYFP-marked CBCD34 cells

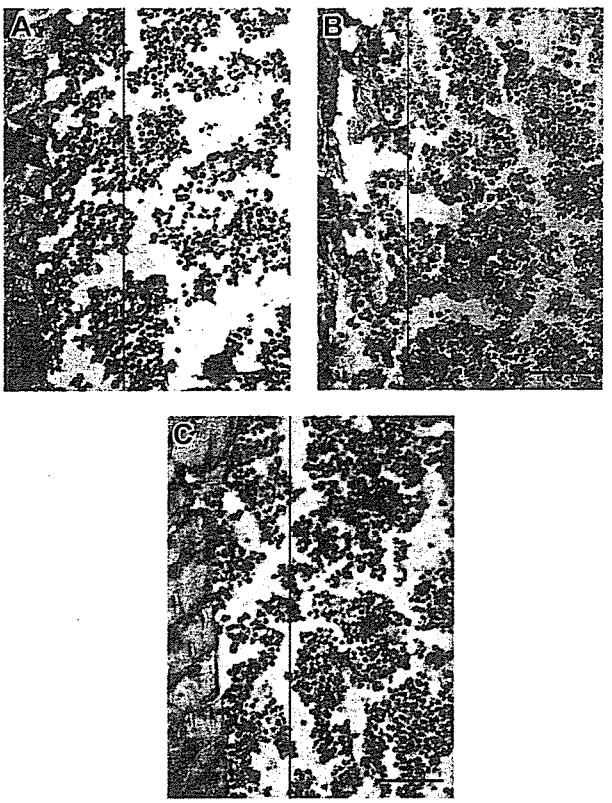

Figure 1. Spatial distribution of human hematopoietic cells in the murine BM compartment. Representative pictures of bone specimens from NOD/SCID mice at 10 weeks after IBMT of 2×10^5 CBCD34 cells are shown. Slides were stained with either anti-CD34, anti-CD15, or anti–glycophorin A antibody, and cells expressing the respective antigens were distinguished by brown reactive products of DAB on immunohistochemistry. $CD34^+$ cells are localized to the endosteal region (A; black arrowheads), whereas $CD15^+$ (B) and $GlyA^+$ cells (C) are distributed away from the endosteum. Vertical lines demarcate 12 cells of the endosteum. Bars represent 100 μm. Images were obtained using an Olympus AX80 microscope and a 20 ×/0.7 NA UPlanApo objective lens. Images were captured using a DP50 digital camera fitted with Viewfinder Lite (all from Olympus, Tokyo, Japan).

(eYFP-CBCD34; Figure 2A) or eGFP-marked MSCs (eGFP-MSCs; Figure 2B). When excess numbers of eYFP-CBCD34 cells (2×10^5) were transplanted intravenously or by IBMT, similar amounts of $eYFP^+$ human hematopoietic cells (eYFP-cells) that expressed human CD45, a pan-leukocyte marker, were observed in BM at both time points examined (Figure 2C-D and data not shown). In marked contrast to the sufficient engraftment of human hematopoietic cells, intravenous administration of 1×10^6 eGFP-MSCs resulted in virtually no visible MSCs in BM at either 4 (Figure 2F) or 10 weeks after transplantation. At 10 weeks after transplantation, analysis of 250 bone sections prepared from 5 mice yielded a total of only 10 eGFP-MSCs in BM. However, when the same number of MSCs was administered by IBMT, eGFP-MSCs were clearly identified in BM at the both time points. At 4 weeks after transplantation, eGFP-MSCs were broadly distributed in BM (Figure 2G-H). At 10 weeks after transplantation, eGFP-MSCs were detected in all sections examined (> 1000 sections), although the number of eGFP-MSCs per section varied considerably (range, 1-57; median, 13; mean, 14.8; from 91 sections) depending on the plane of sectioning. Interestingly, unlike eYFP-cells, which migrated into the contralateral tibia,[12] no eGFP-MSCs were detected in the BM of the tibia that had not received injections (data not shown), suggesting no or minimal migration of transplanted MSCs in this system.

Table 1. Spatial distribution of human hematopoietic cells in the murine BM compartment at 10 weeks after IBMT of CBCD34

	Total no. cells counted	Total no. cells in the endosteal region	Cells in the endosteal region/slide, %
CD34	1469	1086	71.4 ± 12.5*
CD15	2940	451	14.9 ± 6.2
GlyA	1514	171	10.7 ± 2.2

Fourteen slides from at least 8 different mice were examined to count each cell type. Slides containing 115 ± 19 cells in the diaphyseal shaft were chosen for this analysis. Because the endosteal region was arbitrarily decided within 12 cells of both endosteum, the endosteal area comprised approximately 21.4% ± 3.8% of the BM cavity in this study. The proportion of cells located in the endosteal area was calculated for each slide and expressed as the means ± SD.

*$P < .001$ relative to the CD15 and GlyA groups.

Integration of human MSCs into the murine microenvironment

Having confirmed the effectiveness of delivering MSCs into BM, IBMT was used for all subsequent experiments. The phenotypes of transplanted MSCs and their progeny at 10 weeks after transplantation were investigated in detail. In contrast to the bone specimens prepared at 4 weeks after transplantation, in which eGFP-MSCs were located throughout the marrow cavity (Figure 2G-H), eGFP-MSCs at 10 weeks after transplantation were preferentially localized to the endosteal region (73.8% ± 18.4%, n = 251 eGFP-MSCs), frequently within 5 cells from the surface of the bone. When human MSC-derived eGFP-expressing cells (eGFP-cells) were found away from the endosteum, they were often associated with the vasculature (Figure 3A,D). Those vasculature-associated eGFP-cells expressed α-SM actin (Figure 3B-C,E-F), the expression of which has been documented in pericytes, SM cells of the vascular wall as well as myofibroblasts in BM.[23,24] A total of 59.9% ± 21.6% of eGFP-cells (n =251) found in BM were positive for α-SM actin.

Two other types of eGFP-cells that were negative for α-SM actin were also present in BM: flattened cells located in the hematopoietic cords but not specifically associated with the vasculature (Figure 3G) and cells characterized by long cytoplasmic extensions, so-called reticular cells (Figure 3H) that are considered to be the predominant cells of the HME.[25,26] BM was often interspersed with a fine network of cell processes that expressed alkaline phosphatase (ALP; Figure 3I), an enzyme that distinguishes reticular cells from the stromal component of acid phosphatase– or nonspecific esterase–expressing macrophages.[11,25] A total of 28.2% ± 11.2% of eGFP-cells (n = 242) in BM were ALP$^+$.

In addition, eGFP-cells were found within or on the surface of the bone (Figure 3J-O). Cells in the bone stained positive for osteocalcin, a specific marker of mature osteoblasts and osteocytes (Figure 3K-L), indicating an active participation in skeletal remodeling.[27,28] Interestingly, eGFP-cells on the bone surface resembled spindle-shaped osteoblasts (Figure 3M; see also Figure 7), a key component of the stem cell niche in murine hematopoiesis.[29-32] These cells expressed osteopontin (data not shown) and N-cadherin (Figure 3M-O), both of which are involved in regulating murine HSCs.[29,33,34] In a small number of mice examined (4 of 39), eGFP-cells associated with the vasculature stained positive for CD31 (Figure 3P-R) and CD34 (Figure 3S-U), markers of endothelial cells. MSCs expanded ex vivo prior to transplantation did not react with any of these markers either by the immunohistochemical or flow cytometric method, but they did stain positive for vimentin, a marker of fibroblasts (data not shown). These results indicate that within 10 weeks after transplantation, human MSCs differentiated into pericytes, myofibroblasts, reticular cells, osteocytes in bone, bone-lining osteoblasts, and endothelial cells, which constitute the 3-dimensional structure of hematopoietic parenchyma and provide the milieu of hematopoiesis.[26] Therefore, we designated these cells as human MSC-derived hematopoietic microenvironment reconstituting cells (HMRCs).

Engraftment of human hematopoietic cells

During analysis of the engraftment and differentiation of transplanted MSCs, we frequently observed physical contact between HMRCs and hematopoietic eYFP-cells (Figure 3A-I). In particular, eYFP-cells were intimately associated with ALP$^+$ eGFP-reticular cells, where eYFP-cells were almost surrounded by the thin delicate cytoplasm of the eGFP-reticular cells (Figure 3H-I). To address whether the presence of HMRCs in the murine HME contributes to the development of human hematopoietic cells, we analyzed the engraftment and differentiation of CBCD34 cells after transplantation with or without human MSCs. MSCs were injected into the right tibiae of irradiated NOD/SCID mice by IBMT, and then CBCD34 cells were administered intravenously into each mouse. Consistent with our histologic findings, more human CD45$^+$ cells were found in the tibiae into which MSCs had been injected than the tibiae that had not received injections. In addition, the presence of MSCs increased the percentage of CD34$^+$ cells

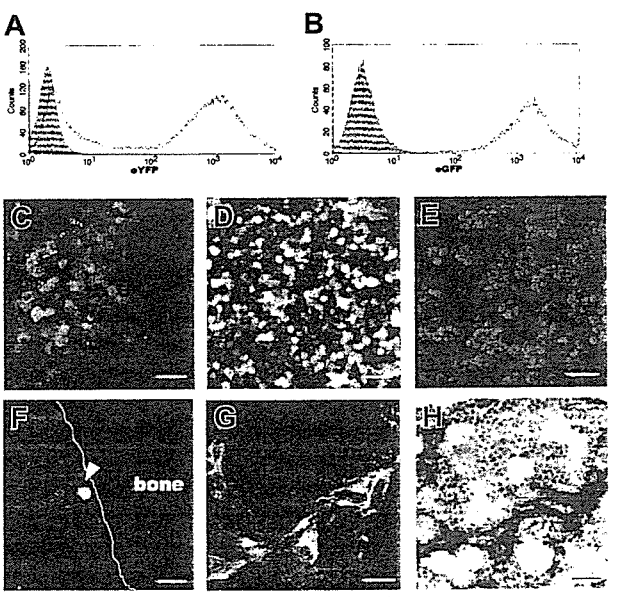

Figure 2. In situ visualization of human MSCs and hematopoietic cells in the murine BM compartment at 4 weeks after IBMT or intravenous transplantation. Transduction efficiencies of eYFP into CBCD34 cells and eGFP into MSCs, determined by flow cytometric analysis at the day of transplantation, were approximately 65% (A) and 99% (B), respectively. The shaded histograms indicate nontransduced cells. (C-E) The presence of human hematopoietic cells was determined by eYFP fluorescence and immunofluorescence staining with an anti–human CD45 antibody followed by Alexa-fluor 594 goat anti–mouse immunoglobulin secondary antibody. Cell nuclei were visualized by staining with TOTO3. Similar amounts of eYFP-cells expressing human CD45 (red) are present in BM after intravenous transplantation (C) or IBMT (D). (E) No eYFP- or CD45-reactive cells are present in the BM of noninjected mouse. (F) eGFP-MSCs are rarely seen in BM after intravenous transplantation (white arrowhead). After IBMT, eGFP-MSCs are easily identified in the BM cavity by eGFP fluorescence (G) and immunohistochemistry (H). (G-H) The same section was stained with an anti-GFP antibody after examining for eGFP fluorescence. All bars represent 10 μm. Images in panels C-G were obtained using an LSM510 META confocal microscope; image in panel H was obtained using an Olympus AX80 microscope and a 20 ×/0.7 NA UPlanApo objective lens.

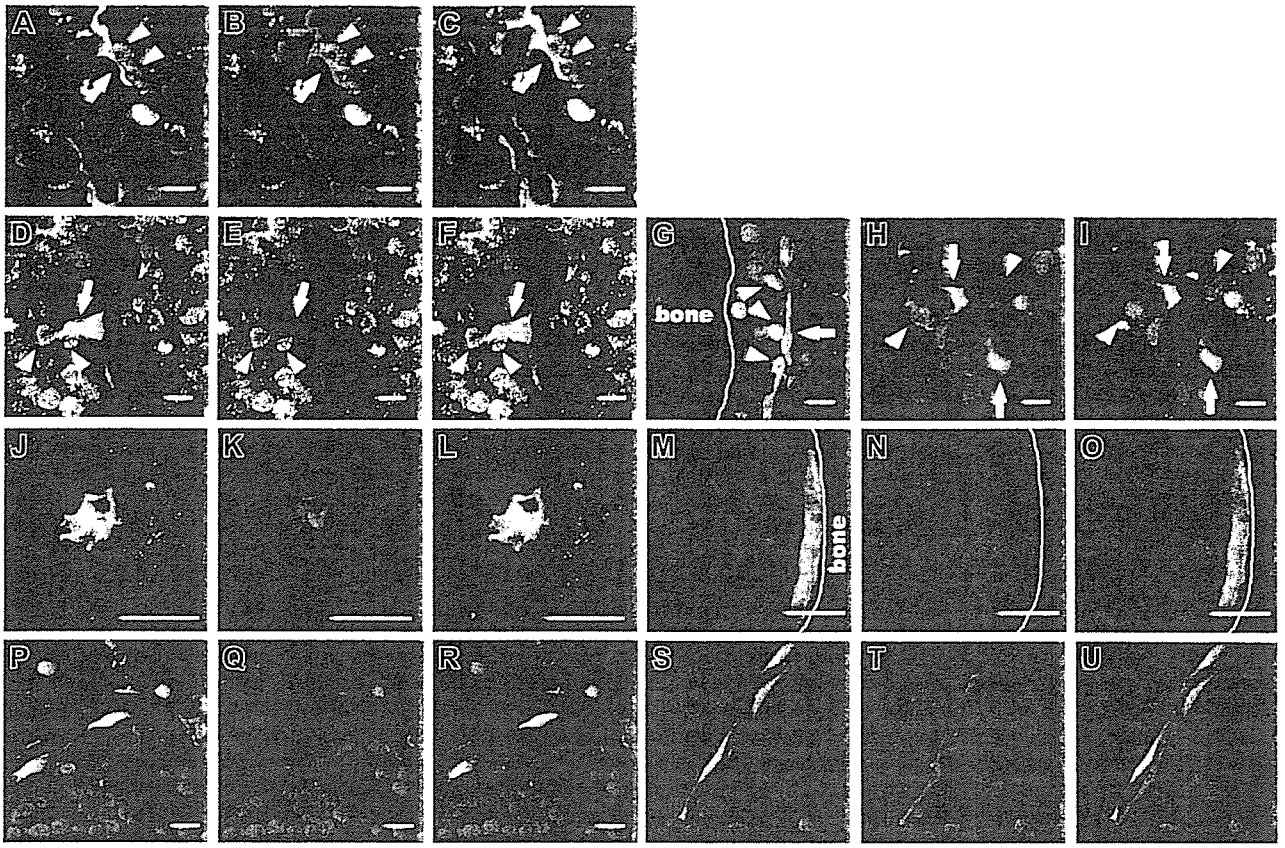

Figure 3. Site-specific differentiation of human eGFP-MSCs in the murine BM compartment. The engraftment and differentiation of transplanted eGFP-MSCs were determined by eGFP fluorescence and immunofluorescence staining for lineage-specific antigens. eGFP-cells were located on the abluminal side of endothelial cells (A) or lined the sinus wall (D). Those vasculature-associated eGFP-cells express α-SM actin (red in panels B and E, and merged in panels C and F). (A-F) eYFP-cells reside next to eGFP-cells. (G) An elongated cell in the endosteal hematopoietic cord interacts with eYFP-cells. eGFP-reticular cells (H) with ALP$^+$ (red) cytoplasmic extensions (I), which haphazardly radiate into the hematopoietic parenchyma, interact with eYFP-cells. An eGFP-cell in the bone exhibits the morphology of authentic osteocytes with filopodial processes surrounded by bone matrix and extending into the canaliculi (J), and expresses osteocalcin (red, K-L). A bone-lining eGFP-cell (M) expresses N-cadherin (red, N-O). N-cadherin is localized to the cell surface. Vasculature-associated eGFP-cells (P,S) express CD31 (red, Q-R) and CD34 (red, T-U). Interactions between eGFP-cells (arrows) and eYFP-cells (arrowheads in A-I) are seen in the specimens from mice in which eGFP-MSCs and eYFP-CBCD34 were cotransplanted. All bars represent 10 μm.

without affecting the proportion of CD19$^+$ B lymphocytes or CD33$^+$ myeloid cells (Figure 4A). There were 2-fold more human CD45$^+$ cells in the tibiae into which MSCs had been injected compared with the tibiae that had not received injections (25.7% ± 17.6% versus 12.8% ± 11.1%, $P = .002$, Figure 4B), and the absolute number of CD34$^+$ cells present in the tibiae into which MSCs had been injected was 3-fold higher than that in the tibiae that had not received injections (99 296 ± 68 189 versus 31 525 ± 25 224; $P = .007$, Figure 4C). Control experiments, in which the same volume of PBS was injected into the right tibia, were conducted to exclude the possibility that this effect was due to injury from the injection. There were no significant differences in either the percentage of CD45$^+$ cells or the number of CD34$^+$ cells between the tibiae into which PBS had been injected and the contralateral tibiae (Figure 4B-C). We then examined the colony-forming ability of BM cells recovered from the mice that had received injections of MSCs and control mice given PBS. The cumulative numbers of colony-forming cells (CFCs) recovered from both tibiae of experimental animals were 2663 for the group that had received injections of MSCs and 1578 for the control group (n = 3 for each group). The proportion of colony types formed from BM cells obtained from both groups was similar (data not shown). Because the numbers of CFCs recovered from each experimental animal varied considerably, we compared the proportion of CFCs present in the tibiae into which MSCs had been injected with the tibiae that had not received injections over the total number of CFCs in each animal. In mice given MSCs, the tibiae into which MSCs had been injected contained the majority of CFCs (89.4% ± 6.7% versus 10.6% ± 6.7%, $P = .007$), whereas CFCs were evenly distributed in the right and left tibiae (53.3% ± 18.1% and 46.7% ± 18.1%, respectively) in control mice (Figure 4D). These results confirmed that the presence of human MSCs positively affected the engraftment of human HSCs.

To assess if there were any functional differences between human cells engrafted in the tibiae into which MSCs had been injected and tibiae that had not received injections, we transplanted BM cells obtained from each tibia of primary mice to separate secondary hosts. Two of 3 secondary host pairs showed human cell engraftment. A pair of recipients, which received cells from the primary host with minimal engraftment (CD45% content; 1.44% for tibiae into which MSCs had been injected and 0.52% for tibiae that had not received injections), failed to show engraftment. As expected, secondary hosts that received BM cells of the tibiae into which MSCs had been injected demonstrated a markedly higher level of engraftment than the hosts that received cells of tibiae that had not received injections (Figure 4E). Taken together, the presence of HMRCs in murine BM augmented not only the proportion of human cells but also the function of human cells engrafted in mouse BM.

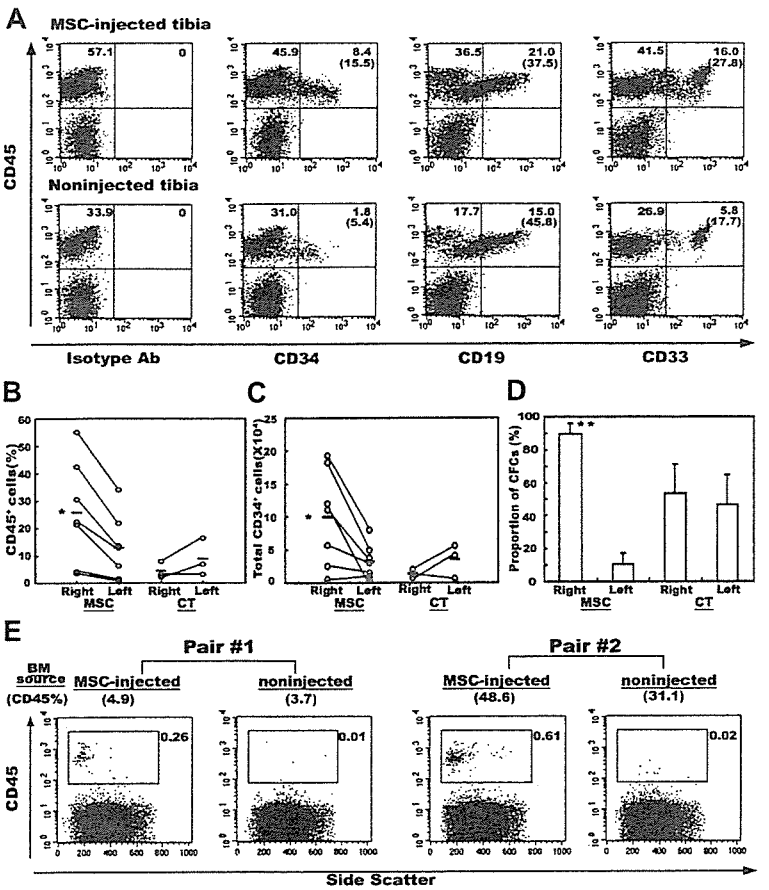

Figure 4. Effect of human MSCs on the engraftment of human hematopoietic cells. (A) BM cells obtained from the MSC-injected or noninjected tibia from the same mouse were examined by flow cytometry at 6 weeks after transplantation. Representative flow cytometric profiles are shown. The relative frequencies of each population are shown at the corner of the respective quadrants. The numbers in parentheses indicate the proportion of $CD45^+$ cells positive for each marker. (B) Percentages of human $CD45^+$ cells in the right (injected) and the left (noninjected) tibia of the MSC-injected (MSC) and control mice (CT). (C) Absolute numbers of $CD34^+$ cells in the right and the left tibia of the MSC-injected and control mice. Each white circle represents one mouse. Values obtained from the same mouse are connected with lines. (D) Distribution of clonogenic progenitors into the right and the left tibia of the MSC-injected and control mice. The proportions of clonogenic cells present in the respective tibia over the total number of clonogenic cells recovered from both tibiae of each mouse are shown (n = 3). $^*P < .05$ and $^{**}P < .01$ relative to the noninjected (left) tibia. (E) Secondary transplantation. BM cells obtained separately from the MSC-injected or noninjected tibia from the same mouse were transplanted into separate secondary hosts. Human cell engraftment was analyzed by CD45 expression at 6 weeks after transplantation. Results of 2 pairs of secondary host are shown. Numbers in parentheses above each flow cytometric profile show the percentage of CD45 cells in the BM cells of primary host. The relative frequencies of CD45 cells in secondary hosts are shown in each profile.

Interaction between human MSC-derived cells and human hematopoietic cells

Having shown the effect of MSCs on human hematopoietic cell engraftment, we examined the underlying basis of increased engraftment in phenotypically and functionally primitive cells. First, we asked whether MSCs play a role in the migration and homing of HSCs to BM, critical steps in the engraftment and initiation of hematopoiesis after transplantation. Prior to intravenous administration of CBCD34, each mouse was given injections of MSCs into the right tibia and PBS into the left tibia. The percentages of CBCD34 cells homed to the tibiae into which MSCs and PBS had been injected were not different (0.05% ± 0.02% and 0.04% ± 0.01%, respectively; n = 3). Thus, MSCs did not seem to function in the initial homing of CBCD34 cells.

We then asked whether MSCs participate in the repopulation process of human hematopoietic cells in the murine HME. At 10 weeks after transplantation, human MSC-derived HMRCs and CBCD34-derived hematopoietic cells frequently interacted (Figure 3), suggesting the role of HMRCs in the maintenance of human hematopoiesis. When those hematopoietic cells were immunophenotyped, $CD34^+$ cells were often in contact or within close proximity to HMRCs (Figure 5Ai), contrasting to lineage-committed $CD15^+$ and $GlyA^+$ cells that were usually found away from HMRCs (Figure 5Aii-iii). Interestingly, one HMRC interacted with 7 $CD34^+$ cells (Figure 5Aiv). These results suggest that HMRCs interact specifically with primitive human hematopoietic cells; therefore, we quantitated HMRCs that were in physical contact with $CD34^+$, $CD15^+$, or $GlyA^+$ cells (Table 2; Figure 5B). Whereas approximately half of all HMRCs in BM were in contact with $CD34^+$ cells, less than 4% of HMRCs were in contact with the lineage-committed cells (Figure 5Bi). Furthermore, the vast majority of HMRCs located in the endosteal region interacted with $CD34^+$ cells (Figure 5Bii). We then examined the human hematopoietic cells that were in contact with HMRCs. A significantly higher proportion of $CD34^+$ cells interacted with HMRCs compared to the lineage-committed cells (Figure 5Biii). The proportion of $CD34^+$ cells interacting with HMRCs in the endosteal region was 2-fold higher than that of $CD34^+$ cells in the central marrow (Figure 5Biv). The result suggests that $CD34^+$ cells in the endosteal region and the central marrow represent different populations of $CD34^+$ cells.

Because the heterogeneity among $CD34^+$ stem/progenitor cells is known,[35-39] we further examined the interaction between $CD34^+$ cells and HMRCs by transplanting SRC-enriched $CD34^+CD38^-$ cells or more mature $CD34^+CD38^+$ progenitor cells together with MSCs (Figure 6). At 1 week after transplantation, there were no differences in the proportions of $CD34^+$ cells localized to the endosteal region (27.4% ± 7.8% for the $CD34^+CD38^-$ group and 26.5% ± 12.1% for the $CD34^+CD38^+$ group) or $CD34^+$ cells interacting with HMRCs (8.1% ± 10.2% and 8.2% ± 9.7%, respectively) between the 2 experimental groups. At 3 weeks after transplantation, the proportion of $CD34^+$ cells in the endosteal area was 2-fold higher in the group that had received transplants of SRC-enriched $CD34^+CD38^-$ cells (63.3% ± 7.9% versus 33.1% ± 8.3%; $P < .001$). To our interest, a significantly higher proportion of $CD34^+$ cells were in contact with HMRCs in the group that had received transplants of $CD34^+CD38^-$ cells (9.4% ± 4.8% versus 4.4% ± 4.0%; $P < .05$). In the group that

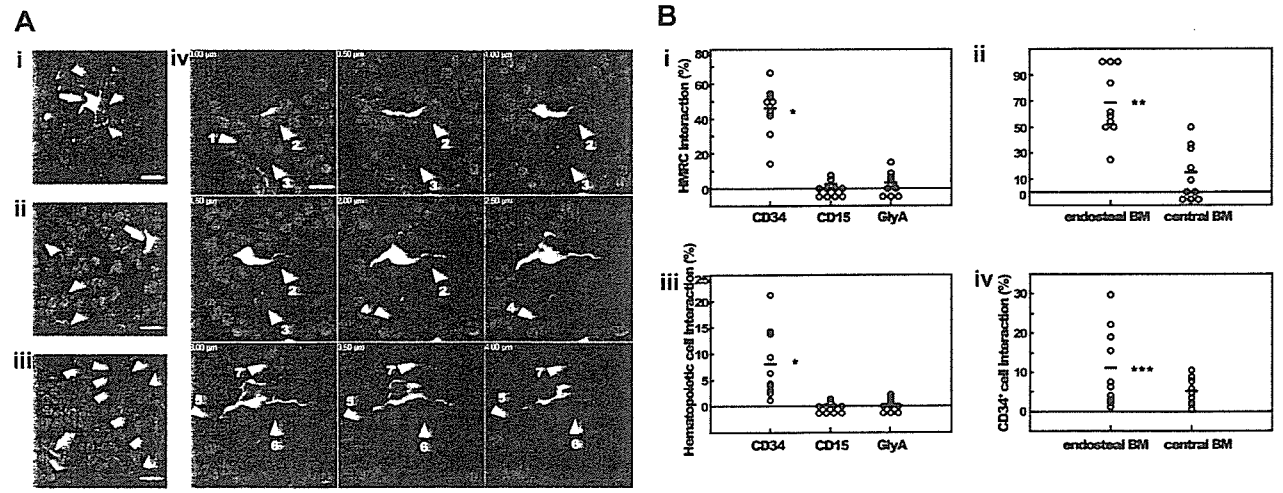

Figure 5. Interaction between HMRCs and CD34$^+$, CD15$^+$, or GlyA$^+$ cells. (A) Bone slides were stained with either anti-CD34, anti-CD15, or anti–glycophorin A antibody followed by Alexa-fluor 594 goat anti–mouse immunoglobulin secondary antibody, and examined under fluorescent microscope. (Ai) CD34$^+$ cells are in physical contact with the cell body and cytoplasmic extensions of a HMRC. CD15$^+$ (Aii) or GlyA$^+$ cells (Aiii) are not found close to HMRCs. HMRCs and immunophenotyped cells are indicated by arrows and arrowheads, respectively. (Aiv) One HMRC in the hematopoietic parenchyma interacts with 7 CD34$^+$ cells (numbered arrowheads). Numerical letters at the left corner of each panel indicate the position of z-axis in the analytical planes. All bars represent 10 μm. (B) Quantification of the interaction between HMRCs and CD34$^+$, CD15$^+$, or GlyA$^+$ cells. (Bi) Frequencies of HMRCs interacting with CD34$^+$, CD15$^+$, or GlyA$^+$ cells. (Bii) The vast majority of HMRCs located in the endosteal region interact with CD34$^+$ cells. (Biii) Frequencies of CD34$^+$, CD15$^+$, or GlyA$^+$ cells interacting with HMRCs. (Biv) In the endosteal region, 2-fold more CD34$^+$ cells interact with HMRCs than in the central marrow. Each white circle represents a value obtained by counting. *$P < .005$ relative to the CD15 and GlyA groups; **$P < .005$ and ***$P < .05$ relative to the central group.

had received CD34$^+$CD38$^+$ transplants, CD34$^+$ cells interacting with HMRCs became progressively rarer (8.2% ± 9.7% at 1 week and 4.4% ± 4.0% at 3 weeks) and were rarely observed at 6 weeks after transplantation (1.1% ± 1.0%). At both time points examined, the group that had received CD34$^+$CD38$^-$ transplants contained higher proportions of CD34$^+$ cells interacting with bone-lining osteoblasts (9.3% ± 10.9% versus 2.7% ± 5.5% at 1 week and 32.4% ± 16.8% versus 17.4% ± 9.9% at 3 weeks). This tendency of CD34$^+$CD38$^-$ cells, the preferential localization of CD34$^+$ cells in the endosteal area and their interaction with bone-lining osteoblasts, may reflect their high repopulation potential. In another words, SRC-enriched CD34$^+$CD38$^-$ cells localize to the endosteal area and interact with bone-lining osteoblasts as well as HMRCs, and progressively become distant to the endosteal area as they differentiate into progenitor cells and finally to mature cells. These results confirmed our earlier observation that HMRCs interacted with the primitive population of CD34$^+$ cells, which resulted in the enhanced engraftment of human hematopoietic cells.

Molecular interaction of HMRCs and CD34$^+$ cells

To determine how HMRCs participated in human hematopoietic cell repopulation in mice, we investigated the molecular interaction of HMRCs and CD34$^+$ cells. We found that CD34$^+$ cells adhered to HMRCs on the bone surface and appeared to proliferate along the endosteal surface, suggesting the existence of specific local signals between CD34$^+$ cells and bone-lining HMRCs (Figure 7A). Double staining for N-cadherin and CD34 demonstrated that bone-lining HMRCs associated with CD34$^+$ cells through the colocalization of N-cadherin (Figure 7B-E). In addition, an HMRC in the endosteal hematopoietic parenchyma expressed stromal cell-derived factor 1 (SDF-1) and interacted with a few eYFP-human hematopoietic cells (Figure 7F-H), although SDF-1 was not detected in ex vivo expanded MSCs by immunofluorescence analysis (data not shown). In BM, SDF-1 is constitutively expressed by osteoblasts, endothelial cells, and BM stromal cells.[40] In addition to its well-established role in homing and retention of HSCs in BM,[41] SDF-1 has been implicated

Table 2. Interactions between HMRCs and human hematopoietic cells at 10 weeks after IBMT of eGFP-MSCs plus CBCD34

	HMRC interaction with hematopoietic cells			Hematopoietic cell interaction with HMRC		
		HMRCs interacting			Hematopoietic cells interacting	
	No. cells counted	Total no.	Frequency, %	No. cells counted	Total no.	Frequency, %
CD34						
Total	150	66	45.9 ± 13.5*	1609	76	8.0 ± 6.2*
Endosteal	81	49	68.0 ± 24.8†	1012	59	11.0 ± 9.4‡
Central	59	17	14.6 ± 17.9	597	17	5.0 ± 3.1
CD15	100	3	1.2 ± 2.4	2603	3	0.14 ± 0.28
GlyA	154	5	3.2 ± 4.5	1624	5	0.36 ± 0.49

BM sections stained with either anti-CD34, anti-CD15, or anti–glycophorin A (GlyA) antibody were examined under fluorescent microscope (10 slides from at least 5 different mice for each cell type). The total numbers of HMRCs and immunophenotyped hematopoietic cells present in the sections were counted, and individual cells were examined for physical contact between HMRCs and hematopoietic cells. Proportions of interacting cells/slide were calculated for each cell type and expressed as the means ± SD. Interactions in CD34$^+$ cell group were further categorized into the endosteal and the central BM groups based on the histoanatomic location of cells.

*$P < .005$ relative to the CD15 and GlyA groups.

†$P < .005$ relative to the central group.

‡$P < .05$ relative to the central group.

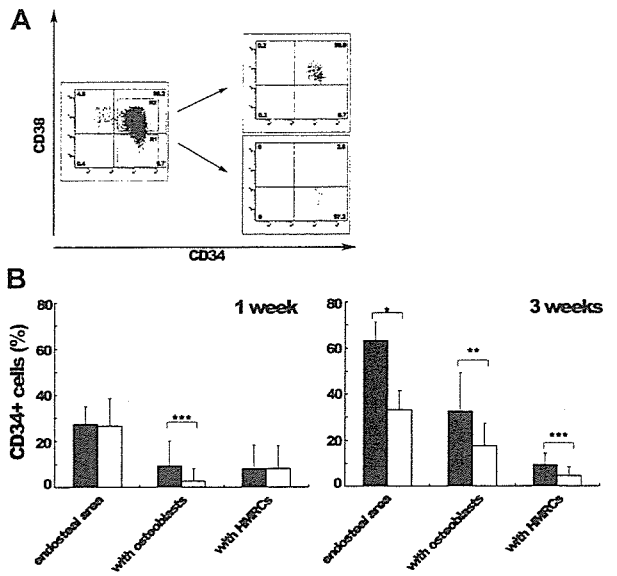

Figure 6. In vivo localization of CD34⁺ cells and their interaction with HMRCs after IBMT of CD34⁺CD38⁻ or CD34⁺CD38⁺ populations together with human MSCs. (A) Sorting profiles of CD34⁺CD38⁺ and CD34⁺CD38⁻ populations. The relative frequencies of each population are shown in the corner of the respective quadrants. (B) At 1 or 3 weeks after IBMT, bone sections were stained with an anti-CD34 antibody and examined for counting. Eighteen slides from 3 mice for each group were counted to obtain the proportion of CD34⁺ cells localized to the endosteum (endosteal area) at the both time points. CD34⁺ cells in the endosteal area were further categorized into cells attaching to bone-lining osteoblasts (with osteoblasts) and cells interacting with HMRCs (with HMRCs). The proportions of CD34⁺ cells in each category are shown. At 1 week after IBMT, the proportions of CD34⁺ cells both in the endosteal area and in contact with HMRCs were not different between the 2 groups. At 3 weeks after IBMT, the SRC-enriched CD34⁺CD38⁻-transplanted group had the higher proportions of CD34⁺ cells in the endosteal area as well as those interacting with HMRCs. At the both time points examined, the proportion of CD34⁺ cells interacted with osteoblasts was higher in the SRC-enriched CD34⁺CD38⁻-transplanted group. Bars represent the CD34⁺CD38⁻-transplanted group (■) and the CD34⁺CD38⁺-transplanted group (□). $^{*}P < .001$, $^{**}P < .005$, and $^{***}P < .05$ relative to the CD34⁺CD38⁺ group.

in regulating the status of primitive HSCs both in vitro and in vivo.[42-44] Therefore, HMRCs may contribute to the maintenance of primitive human HSCs through N-cadherin–mediated interactions and the production of SDF-1.

Discussion

Our study demonstrated that intramedullary transplanted human MSCs reconstituted the HME and provided direct evidence for a role of transplanted human MSCs in the enhancement of human hematopoietic cell repopulation in mice. The initial histologic analysis unveiled the integration of human hematopoietic cells into the specially and functionally compartmentalized HME of NOD/SCID mice. Based on this finding, we established a model system that enables the identification of the phenotype and function of human MSCs in vivo by directly injecting genetically marked human MSCs into the BM of NOD/SCID mice. Analogous to human HSCs, human MSCs persisted long-term in murine BM to at least 10 weeks after transplantation and were able to differentiate into the key components of the HME in the host. The presence of human MSCs in murine BM correlated with the increase in human hematopoietic cells that were phenotypically and functionally primitive. Engrafted human MSCs appeared to be involved in the maintenance of human hematopoiesis via secreted factors as well as by physically interacting with primitive hematopoietic cells.

The stem cell niche is a key determinant of stem cell development.[45,46] We are beginning to understand the murine HSC niche and the molecular mechanisms that govern the fate of murine HSCs,[47] but there exists a paucity of data on the cellular and molecular microenvironmental regulation of human hematopoiesis in vivo due largely to a lack of good experimental tools. Although the identification of SRCs has facilitated detailed characterization of human HSCs in vivo,[20,48] the key niches that function in human cell repopulation have not been identified. Our study has demonstrated for the first time that CD34-expressing stem/progenitor cells localize to the endosteal surface and mobilize toward the central marrow as they differentiate in BM. In addition, SRC-enriched CD34⁺CD38⁻ cells demonstrated a distinct trend to localize in the endosteal region and to interact with bone-lining osteoblasts, even at the early stage of hematopoietic reconstitution. This may be one of the reasons that CD34⁺CD38⁻ cells have the high repopulation potential. We also found that human MSC-derived HMRCs locally created human HME in the murine environment. Visualization of human hematopoietic cells and human HMRCs in situ made it possible to elucidate the physical interaction between human hematopoietic cells and the human microenvironment. In this way, the SRC assay recapitulates human hematopoiesis in the murine environment both structurally and functionally and could serve as a good experimental system to study human hematopoiesis.

The presence of human MSCs in murine BM resulted in significantly more engraftment of phenotypically and functionally primitive human hematopoietic cells. With this newly established experimental system, we were able to present 3 lines of evidence that explain how human MSCs may facilitate human hematopoietic cell engraftment. First, the interaction of human MSC-derived HMRCs and human CD34⁺ cells was mostly observed in the

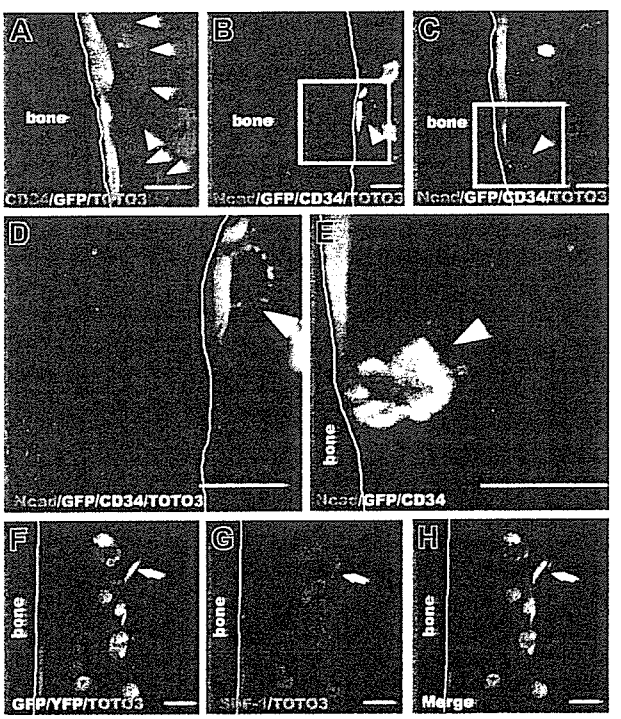

Figure 7. Expression of N-cadherin and SDF-1 by HMRCs that interact with human hematopoietic cells. (A) CD34⁺ cells (arrowheads) appear to colonize near the bone-lining HMRCs. (B-C) Bone-lining HMRCs colocalize with CD34⁺ cells (arrowheads) through the asymmetrical expression of N-cadherin. (D-E) Higher magnifications of panels B and C. (F-H) An HMRC in the endosteal hematopoietic parenchyma (arrow) expresses SDF-1 and interacts with a few eYFP hematopoietic cells. All bars represent 10 μm.

endosteal region, at a significantly higher frequency than that of lineage-committed cells. When this interaction was examined further by using sorted populations of SRC-enriched $CD34^+CD38^-$ cells and more mature $CD34^+CD38^+$ progenitor cells, a preferential interaction of HMRCs with a primitive population of $CD34^+$ cells was evident. Whereas the proportion of $CD34^+$ cells interacting with HMRCs rapidly decreased in the group that had received $CD34^+CD38^+$ progenitor cells, this frequency in the group that had received $CD34^+CD38^-$ transplants did not change and was equivalent to the proportion of $CD34^+$ cells interacting with HMRCs at 10 weeks after transplantation. Considering that the proportion of $CD34^+CD38^-$ cells originally contained in the $CD34^+$ cells (representing 5%-8% of $CD34^+$ cells in this study) was similar to HMRC-interacting $CD34^+$ cells ($8.0\% \pm 6.2\%$ at 10 weeks), transplanted human MSCs, which became an integral part of the functional HME, interacted with primitive cell populations, provided supportive environment of human hematopoiesis, and augmented human cell engraftment. Second, bone-lining HMRCs interacted with $CD34^+$ cells through the asymmetric expression of N-cadherin, similar to the way bone-lining osteoblasts maintain primitive HSCs in mouse. This specific interaction of $CD34^+$ cells with human MSC-derived bone-lining osteoblasts, a cellular component of the stem cell niche, indicates that similar regulatory mechanisms operate in human and murine hematopoiesis. Third, HMRCs in the endosteal hematopoietic parenchyma produced SDF-1 and interacted with human hematopoietic cells. This strengthens the previous observations that SDF-1 regulates the proliferation and survival of primitive HSCs and progenitor cells.[12,42-44] Taken together, these results suggest that human MSC-derived HMRCs contribute not only to the proliferation and differentiation of human hematopoietic progenitor cells that results in the increased chimerism but also to the maintenance of primitive human HSCs.

Embryonic development is strictly regulated through sequential and concerted events that are orchestrated by interactions between tissue stem cells and the microenvironment. This developmental paradigm, including signaling molecules that regulate stem cell self-renewal,[49] is conserved for generating and maintaining specific tissues in adult life, and dysregulation of this process leads to pathologic conditions such as cancer.[50] Current empiric cancer studies have focused on identifying intrinsic genetic changes that lead to the aberrant proliferation of cells, and, as a result, therapeutic agents targeting the genetic mutations are emerging. However, our understanding of extrinsic, or microenvironmental, signals in the context of tumorigenesis has lagged behind. Because the microenvironment is responsible for homeostatic controls,[45,51,52] is there a specific microenvironment that permits, initiates, or complements tumorigenesis and supports progression of tumors? Could the microenvironment be a new target for cancer therapy? The experimental system we described here, which allows the visualization and reconstitution of a human microenvironment, provides a unique tool to study the maintenance of tissue homeostasis, which may lead to the elucidation of the tumorigenic microenvironment. In addition, the functional persistence of transplanted MSCs in the host environment means that MSCs may be used to deliver therapeutic genes or agents to target tissues.

Acknowledgments

The monoclonal antibody for alkaline phosphatase developed by Dr Katzmann was obtained from the Developmental Studies Hybridoma Bank developed under the auspices of the NICHD and maintained by the University of Iowa, Department of Biological Sciences, Iowa City, IA 52242. The authors thank Dr Hiroyuki Miyoshi, BioResource Center, RIKEN Tsukuba Institute, for providing lentivirus vectors, Hideyuki Matsuzawa and Tamaki Saso for technical assistance, members of Tokai Cord Blood Bank for providing cord blood samples, members of the animal facility of Tokai University for care of experimental animals, and all members of Research Center of Regenerative Medicine for their support.

References

1. Prockop DJ. Marrow stromal cells as stem cells for nonhematopoietic tissues. Science. 1997;276:71-74.
2. Pittenger MF, Mackay AM, Beck SC, et al. Multilineage potential of adult human mesenchymal stem cells. Science. 1999;284:143-147.
3. Conget PA, Minguell JJ. Phenotypical and functional properties of human bone marrow mesenchymal progenitor cells. J Cell Physiol. 1999;181:67-73.
4. Majumdar MK, Thiede MA, Mosca JD, Moorman M, Gerson SL. Phenotypic and functional comparison of cultures of marrow-derived mesenchymal stem cells (MSCs) and stromal cells. J Cell Physiol. 1998;176:57-66.
5. Javazon EH, Beggs KJ, Flake AW. Mesenchymal stem cells: paradoxes of passaging. Exp Hematol. 2004;32:414-425.
6. Koc ON, Gerson SL, Cooper BW, et al. Rapid hematopoietic recovery after coinfusion of autologous-blood stem cells and culture-expanded marrow mesenchymal stem cells in advanced breast cancer patients receiving high-dose chemotherapy. J Clin Oncol. 2000;18:307-316.
7. Noort WA, Kruisselbrink AB, in 't Anker PS, et al. Mesenchymal stem cells promote engraftment of human umbilical cord blood-derived CD34(+) cells in NOD/SCID mice. Exp Hematol. 2002;30:870-878.
8. in 't Anker PS, Noort WA, Kruisselbrink AB, et al. Nonexpanded primary lung and bone marrow-derived mesenchymal cells promote the engraftment of umbilical cord blood-derived CD34(+) cells in NOD/SCID mice. Exp Hematol. 2003;31:881-889.
9. Bensidhoum M, Chapel A, Francois S, et al. Homing of in vitro expanded Stro-1$^-$ or Stro-1$^+$ human mesenchymal stem cells into the NOD/SCID mouse and their role in supporting human CD34 cell engraftment. Blood. 2004;103:3313-3319.
10. Devine SM, Bartholomew AM, Mahmud N, et al. Mesenchymal stem cells are capable of homing to the bone marrow of non-human primates following systemic infusion. Exp Hematol. 2001;29:244-255.
11. Awaya N, Rupert K, Bryant E, Torok-Storb B. Failure of adult marrow-derived stem cells to generate marrow stroma after successful hematopoietic stem cell transplantation. Exp Hematol. 2002;30:937-942.
12. Yahata T, Ando K, Sato T, et al. A highly sensitive strategy for SCID-repopulating cell assay by direct injection of primitive human hematopoietic cells into NOD/SCID mice bone marrow. Blood. 2003;101:2905-2913.
13. Wang J, Kimura T, Asada R, et al. SCID-repopulating cell activity of human cord blood-derived CD34- cells assured by intra-bone marrow injection. Blood. 2003;101:2924-2931.
14. Kawada H, Fujita J, Kinjo K, et al. Nonhematopoietic mesenchymal stem cells can be mobilized and differentiate into cardiomyocytes after myocardial infarction. Blood. 2004;104:3581-3587.
15. Yahata T, Ando K, Miyatake H, et al. Competitive repopulation assay of two gene-marked cord blood units in NOD/SCID/gammac(null) mice. Mol Ther. 2004;10:882-891.
16. Muguruma Y, Reyes M, Nakamura Y, et al. In vivo and in vitro differentiation of myocytes from human bone marrow-derived multipotent progenitor cells. Exp Hematol. 2003;31:1323-1330.
17. Yahata T, Ando K, Nakamura Y, et al. Functional human T lymphocyte development from cord blood $CD34^+$ cells in nonobese diabetic/Shi-scid, IL-2 receptor gamma null mice. J Immunol. 2002;169:204-209.
18. Ito M, Hiramatsu H, Kobayashi K, et al. NOD/SCID/gamma(c)(null) mouse: an excellent recipient mouse model for engraftment of human cells. Blood. 2002;100:3175-3182.
19. Nilsson SK, Johnston HM, Coverdale JA. Spatial localization of transplanted hemopoietic stem cells: inferences for the localization of stem cell niches. Blood. 2001;97:2293-2299.
20. Larochelle A, Vormoor J, Hanenberg H, et al. Identification of primitive human hematopoietic cells capable of repopulating NOD/SCID mouse bone marrow: implications for gene therapy. Nat Med. 1996;2:1329-1337.
21. Lambertsen RH, Weiss L. A model of intramedullary hematopoietic microenvironments based on

stereologic study of the distribution of endocloned marrow colonies. Blood. 1984;63:287-297.

22. Heissig B, Hattori K, Dias S, et al. Recruitment of stem and progenitor cells from the bone marrow niche requires MMP-9 mediated release of kit-ligand. Cell. 2002;109:625-637.
23. Peled A, Zipori D, Abramsky O, Ovadia H, Shezen E. Expression of alpha-smooth muscle actin in murine bone marrow stromal cells. Blood. 1991;78:304-309.
24. Charbord P, Tavian M, Humeau L, Peault B. Early ontogeny of the human marrow from long bones: an immunohistochemical study of hematopoiesis and its microenvironment. Blood. 1996;87:4109-4119.
25. Westen H, Bainton DF. Association of alkaline-phosphatase-positive reticulum cells in bone marrow with granulocytic precursors. J Exp Med. 1979;150:919-937.
26. Lichtman MA. The ultrastructure of the hemopoietic environment of the marrow: a review. Exp Hematol. 1981;9:391-410.
27. Pereira RF, O'Hara MD, Laptev AV, et al. Marrow stromal cells as a source of progenitor cells for nonhematopoietic tissues in transgenic mice with a phenotype of osteogenesis imperfecta. Proc Natl Acad Sci U S A. 1998;95:1142-1147.
28. Nilsson SK, Dooner MS, Weier HU, et al. Cells capable of bone production engraft from whole bone marrow transplants in nonablated mice. J Exp Med. 1999;189:729-734.
29. Zhang J, Niu C, Ye L, et al. Identification of the haematopoietic stem cell niche and control of the niche size. Nature. 2003;425:836-841.
30. Calvi LM, Adams GB, Weibrecht KW, et al. Osteoblastic cells regulate the haematopoietic stem cell niche. Nature. 2003;425:841-846.
31. Arai F, Hirao A, Ohmura M, et al. Tie2/angiopoietin-1 signaling regulates hematopoietic stem cell quiescence in the bone marrow niche. Cell. 2004; 118:149-161.
32. Visnjic D, Kalajzic Z, Rowe DW, Katavic V, Lorenzo J, Aguila HL. Hematopoiesis is severely altered in mice with an induced osteoblast deficiency. Blood. 2004;103:3258-3264.
33. Stier S, Ko Y, Forkert R, et al. Osteopontin is a hematopoietic stem cell niche component that negatively regulates stem cell pool size. J Exp Med. 2005;201:1781-1791.
34. Nilsson SK, Johnston HM, Whitty GA, et al. Osteopontin, a key component of the hematopoietic stem cell niche and regulator of primitive hematopoietic progenitor cells. Blood. 2005;106:1232-1239.
35. Terstappen LW, Huang S, Safford M, Lansdorp PM, Loken MR. Sequential generations of hematopoietic colonies derived from single nonlineage-committed $CD34^+CD38^-$ progenitor cells. Blood. 1991;77:1218-1227.
36. Craig W, Kay R, Cutler RL, Lansdorp PM. Expression of Thy-1 on human hematopoietic progenitor cells. J Exp Med. 1993;177:1331-1342.
37. Yin AH, Miraglia S, Zanjani ED, et al. AC133, a novel marker for human hematopoietic stem and progenitor cells. Blood. 1997;90:5002-5012.
38. Baum CM, Weissman IL, Tsukamoto AS, Buckle AM, Peault B. Isolation of a candidate human hematopoietic stem-cell population. Proc Natl Acad Sci U S A. 1992;89:2804-2808.
39. Murray LJ, Bruno E, Uchida N, et al. CD109 is expressed on a subpopulation of $CD34^+$ cells enriched in hematopoietic stem and progenitor cells. Exp Hematol. 1999;27:1282-1294.
40. Ponomaryov T, Peled A, Petit I, et al. Induction of the chemokine stromal-derived factor-1 following DNA damage improves human stem cell function. J Clin Invest. 2000;106:1331-1339.
41. Lapidot T. Mechanism of human stem cell migration and repopulation of NOD/SCID and B2mnull NOD/SCID mice. The role of SDF-1/CXCR4 interactions. Ann N Y Acad Sci. 2001;938:83-95.
42. Lataillade JJ, Clay D, Dupuy C, et al. Chemokine SDF-1 enhances circulating CD34(+) cell proliferation in synergy with cytokines: possible role in progenitor survival. Blood. 2000;95:756-768.
43. Lataillade JJ, Clay D, Bourin P, et al. Stromal cell-derived factor 1 regulates primitive hematopoiesis by suppressing apoptosis and by promoting G(0)/G(1) transition in CD34(+) cells: evidence for an autocrine/paracrine mechanism. Blood. 2002;99:1117-1129.
44. Cashman J, Clark-Lewis I, Eaves A, Eaves C. Stromal-derived factor 1 inhibits the cycling of very primitive human hematopoietic cells in vitro and in NOD/SCID mice. Blood. 2002;99:792-799.
45. Watt FM, Hogan BL. Out of Eden: stem cells and their niches. Science. 2000;287:1427-1430.
46. Spradling A, Drummond-Barbosa D, Kai T. Stem cells find their niche. Nature. 2001;414:98-104.
47. Taichman RS. Blood and bone: two tissues whose fates are intertwined to create the hematopoietic stem-cell niche. Blood. 2005;105:2631-2639.
48. Guenechea G, Gan OI, Dorrell C, Dick JE. Distinct classes of human stem cells that differ in proliferative and self-renewal potential. Nat Immunol. 2001;2:75-82.
49. Taipale J, Beachy PA. The Hedgehog and Wnt signalling pathways in cancer. Nature. 2001;411: 349-354.
50. Reya T, Morrison SJ, Clarke MF, Weissman IL. Stem cells, cancer, and cancer stem cells. Nature. 2001;414:105-111.
51. Antonchuk J, Sauvageau G, Humphries RK. HOXB4 overexpression mediates very rapid stem cell regeneration and competitive hematopoietic repopulation. Exp Hematol. 2001;29:1125-1134.
52. Mueller MM, Fusenig NE. Friends or foes—bipolar effects of the tumour stroma in cancer. Nat Rev Cancer. 2004;4:839-849.

Direct evidence for ex vivo expansion of human hematopoietic stem cells

Kiyoshi Ando, Takashi Yahata, Tadayuki Sato, Hiroko Miyatake, Hideyuki Matsuzawa, Masayuki Oki, Hiroyuki Miyoshi, Takashi Tsuji, Shunichi Kato, and Tomomitsu Hotta

To characterize human hematopoietic stem cells (HSCs), xenotransplantation techniques such as the severe combined immunodeficiency (SCID) mouse repopulating cell (SRC) assay have proven the most reliable methods thus far. While SRC quantification by limiting dilution analysis (LDA) is the gold standard for measuring in vitro expansion of human HSCs, LDA is a statistical method and does not directly establish that a single HSC has self-renewed in vitro. This would require a direct clonal method and has not been done. By using lentiviral gene marking and direct intra–bone marrow injection of cultured CD34$^+$ CB cells, we demonstrate here the first direct evidence for self-renewal of individual SRC clones in vitro. Of 74 clones analyzed, 20 clones (27%) divided and repopulated in more than 2 mice after serum-free and stroma-dependent culture. Some of the clones were secondary transplantable. This indicates symmetric self-renewal divisions in vitro. On the other hand, 54 clones (73%) present in only 1 mouse may result from asymmetric divisions in vitro. Our data demonstrate that current ex vivo expansion conditions result in reliable stem cell expansion and the clonal tracking we have employed is the only reliable method that can be used in the development of clinically appropriate expansion methods. (Blood. 2006;107:3371-3377)

Introduction

Ex vivo expansion of hematopoietic stem cells (HSCs) is a major challenge for clinical and experimental transplantation protocols.[1-3] Over the past 15 years many investigators have undertaken experiments to study ex vivo expansion of HSCs. These studies have led to a number of clinical trials to evaluate ex vivo–expanded cells in patients. However, no significant clinical benefit has been demonstrated to date. Clonal kinetics of ex vivo–expanded HSCs is one of the basic transplantation biology questions to be addressed before we can optimize ex vivo expansion approaches.

To characterize human HSCs, the severe combined immunodeficiency (SCID) mouse repopulating cell (SRC) assay has proven the most reliable method thus far.[4,5] When this assay was used, the maximal expansion that was achieved was 2- to 4-fold expansion.[6-9] While quantitative SRC assay using limiting dilution analysis (LDA) is the gold standard for measuring expansion, it is a statistical method and does not directly establish that a single HSC has self-renewed in vitro. This would require a direct clonal method and has not been done.

Retrovirus-mediated gene marking has been widely used for clonal analysis. Since these vectors essentially integrate at random, each genomic integration site serves as a distinct clonal marker that can be used to trace the progeny of individual stem cells after transplantation.[10,11] Gene-marking studies in SRC assays have successfully elucidated the in vivo kinetics of human HSCs such as proliferation, self-renewal, and multilineage differentiation.[12,13]

We previously reported serum-free and stroma-dependent (SFSD) culture conditions for the ex vivo expansion of human CD34$^+$ cells using the murine bone marrow stromal cell line HESS-5 and human cytokines Flk-2/Flt-3 ligand (FL), thrombopoietin (TPO), and stem cell factor (SCF).[14,15] To obtain direct evidence that self-renewal division of HSCs in this culture system results in SRC "expansion," we applied lentiviral gene marking and direct intra–bone marrow transplantation (iBMT) of cultured CD34$^+$ cord blood (CB) cells. We demonstrate here the first direct evidence for self-renewal of individual SRC clones in vitro.

Materials and methods

Collection and purification of human CB CD34$^+$ cells

Informed consent was provided according to the Declaration of Helsinki. CB was obtained from full-term deliveries according to procedures approved by the institutional review board of the Tokai University School of Medicine (Kanagawa, Japan). Mononuclear cells (MNCs) were isolated from CB by Ficoll-Hypaque (Lymphoprep, 1.077 ± 0.001 g/mL; Nycomed, Oslo, Norway) density gradient centrifugation. CD34$^+$ cells were purified by positive selection using an immunomagnetic bead system (MACS; Miltenyi Biotec, Glodbach, Germany). More than 95% of the enriched cells were CD34$^+$ cells, as shown by flow cytometric analysis (FACSCalibur; Becton Dickinson, San Jose, CA).

From the Research Center for Regenerative Medicine and the Department of Hematology, Tokai University, School of Medicine, Isehara, Kanagawa; the BioResource Center, Riken Tsukuba Institute, Ibaraki; and the Department of Industrial Science and Technology, Tokyo University of Science, Noda, Chiba, Japan.

Submitted August 3, 2005; accepted December 14, 2005. Prepublished online as *Blood* First Edition Paper, January 3, 2006; DOI 10.1182/blood-2005-08-3108.

Supported by grants from the Ministry of Education, Science, and Culture, Japan; and a Research Grant on Human Genome, Tissue Engineering (H17-014) from the Japanese Ministry of Health, Labor, & Welfare, Tokyo, Japan.

K.A. designed and performed research and wrote the paper; T.Y., T.S., H. Miyatake, H. Matsuzawa, and M.O. performed research; H. Miyoshi and T.T. contributed vital new reagents; S.K. and T.H. analyzed data.

Reprints: Kiyoshi Ando, Department of Hematology, Tokai University School of Medicine Bohseidai, Isehara, Kanagawa 259-1193, Japan; e-mail: andok@keyaki.cc.u-tokai.ac.jp.

The publication costs of this article were defrayed in part by page charge payment. Therefore, and solely to indicate this fact, this article is hereby marked "advertisement" in accordance with 18 U.S.C. section 1734.

Serum-free and stroma-dependent (SFSD) culture system for ex vivo expansion

In this culture system, CB CD34$^+$ cells were physically separated from the stromal layer by a polyethylene-terephthalate track-etched membrane in cell culture inserts (BD Labware, Franklin Lakes, NJ), as previously described.[14] First, the murine hematopoietic-supportive stromal cells HESS-5[16] were cultured on the reverse side of the track-etched membrane of the insert in 12-well microplates in minimal essential medium-alpha (MEM-α; Nikken Bio Medical Laboratory, Kyoto, Japan) supplemented with 10% (vol/vol) horse serum (GibcoBRL) at 37°C under 5% CO_2 in humidified air. Once cells grew to confluency, stromal cells were irradiated with 15 Gy using a ^{137}Cs γ-irradiator, before being washed 5 times with StemPro, and the media changed for coculture. Transduced CB CD34$^+$ cells were seeded on the upper side of the membrane in the insert where the cytoplasmic villi of HESS-5 cells passed through the etched 0.45-μm pores (pore density; 1.0×10^8/cm^2) and were cultured in StemPro TM-34SFM (GibcoBRL) supplemented with StemPro TM-34 Nutrient Supplement (GibcoBRL), 2 mM L-glutamine (GibcoBRL), and penicillin/streptomycin with recombinant human TPO (50 ng/mL; a gift from Kirin Brewery, Tokyo, Japan), SCF (50 ng/mL; a gift from Kirin Brewery) and FL (50 ng/mL; R&D Systems, Minneapolis, MN).

5-and 6-carboxyfluorescein diacetate succinimidyl ester (CFSE) labeling

CFSE labeling of CB CD34$^+$ cells was carried out as described previously.[17] Cells were incubated with 10 μM CFSE (Molecular Probes, Eugene, OR) for 10 minutes at 37°C and then further dye uptake was prevented by washing with cold fetal calf serum (FCS). Labeled cells were cultured in the SFSD system and their kinetics were evaluated using a FACS Calibur (Becton Dickinson).

SRC assay

Male or female NOD/Shi-*scid* (NOD/SCID) mice were obtained from CLEA JAPAN (Tokyo, Japan). All experiments were approved by the animal care committee of Tokai University. Mice were housed in microisolated cages and given autoclaved food and water, acidified just before and after total body irradiation (300 cGy-350 cGy). Mice were anesthetized briefly with ether and injected with transduced cells through the tail vein. After 10 weeks, mice that had undergone transplantation were killed and bone marrow cells were flushed from the femura and tibias with PBS.

iBMT of human hematopoietic cells

iBMT was carried out as previously described.[18] In brief, a 29-gauge needle was inserted into the joint surface of the right tibia of anesthetized mice, and human hematopoietic cells in a 10-μL suspension were injected into the BM cavity. For injections, a 1-mL Hamilton syringe with fixed 31-gauge needle was used.

Lentivirus production and infection of CD34$^+$ cells

The vesicular stomatitis virus–G protein (VSV-G) pseudotyped lentiviral vector was generated by transient cotransfection of the self-inactivating vector construct pCS-CG[19] with the VSV-G–expressing construct pMD.G, the *rev*-expressing construct pRSV, and the packaging construct pMDLg/p.RRE into 293T cells (ATCC, Manassas, VA) using calcium phosphate transfection, according to the manufacturer's recommendations (Invitrogen, Carlsbad, CA). 293T cells were grown on collagen I–coated 100-mm dishes (BD Labware, Bedford, MA) in Dulbecco modified Eagle medium (DMEM; Biofluids, Rockville, MD) containing 10% heat-inactivated FCS (JRH Biosciences, Lenexa, KS). The vector-containing supernatant was collected every 24 hours for 3 days, filtered through a 0.45-μm pore size filter, and superconcentrated twice by centrifugation at 50 000*g* for 90 minutes at 20°C. Viral supernatants were concentrated 100 to 200 times by ultracentrifugation, resuspended in serum-free medium StemPro TM-34SFM, and stored at −80°C until use.

CD34$^+$ cells (100 000) in 200 μL StemPro TM-34SFM were seeded in each well of 96-well V-bottomed plates and cultured for 5 hours with superconcentrated lentiviral supernatant (200 μL/well) at a multiplicity of infection (MOI) of 50.[20]

FACS analysis and sorting

On day 4 after infection, the cells were washed once with PBS and stained with a monoclonal antibody against CD34 conjugated with PE (Becton Dickinson). Infection efficiency was evaluated using a FACS Calibur (Becton Dickinson). At 10 weeks after transplantation, the mice were killed and the bone marrow and spleen were collected. Cells were stained with monoclonal antibodies (mAbs) to human leukocyte differentiation antigens: PE-conjugated anti–human CD19 (SJ25C1) and CD33 (Leu-M9) (all Becton Dickinson); and APC-conjugated anti–human CD45 (J.33; Coulter/Immunotech, Hialeah, FL). A FACS analysis was conducted by 3- or 4-color flow cytometric analysis using a FACSCalibur. For isolation of CD19$^+$EGFP$^+$ and CD33$^+$EGFP$^+$ cells, cells were stained with PE-conjugated anti–human ECD-conjugated CD19 and PE-conjugated CD33, and APC-conjugated anti-CD45 mAbs and sorted using the FACSVantage flow cytometer (BD Biosciences).

3′-LTR integration site analysis using linear amplification-mediated–PCR

To identify the genomic-proviral junction sequence, linear amplification-mediated polymerase chain reaction (LAM-PCR) was performed on DNA isolated from total bone marrow as described by Schmidt et al.[21] In brief, linear amplification of target DNA was performed by repeated primer extension using a vector-specific 5′-biotinylated primer LTR1 (5′ GAA CCC ACT GCT TAA GCC TCA 3′) with Taq polymerase (2.5 U; Qiagen, Valencia, CA) from 100 ng of each sample DNA. After selection with magnetic beads (Dynal, Oslo, Norway), the extension products were incubated with Klenow polymerase (2 U), dNTPs (300 mM; Pharmacia, Uppsala, Sweden), and random hexanucleotide mixture (Takara, Otsu, Japan). The samples were then washed on the magnetic particle concentrator (Dynal) and incubated with Sac I (5 U in 20 μL; Promega, Madison, WI) for 2 hours at 37°C, and then Tsp509 I (5 U in 20 μL; New England BioLabs, Ipswich, MA) for 2 hours at 55°C. After an additional wash step, a double-stranded asymmetric linker cassette and T4 DNA Ligase (6 U; New England BioLabs) were incubated with the beads at 16°C overnight. After denaturing with 0.1 N NaOH, each ligation product was amplified with Taq polymerase (5 U), 25 pmol of vector-specific primer LTR2 (5′ AGC TTG CCT TGA GTG CTT CA 3′), and linker cassette primer LC1 (5′ GTA CAT ATT GTC GTT AGA ACG CGT AAT ACG ACT CA 3′). Of each PCR product, 0.2% served as a template for a second, nested PCR with internal primers LTR3 (5′ AGT AGT GTG TGC CCG TCT GT 3′) and LC2 (5′ CGT TAG AAC GCG TAA TAC GAC TCA CTA TAG GGA GA 3′) under identical conditions. Amplified products were loaded on 2% agarose gels. To quantify the number of each band in cases where several clones of infected cells contributed to the graft, densitometric analysis was done using Densitograph software (ATTO, Tokyo, Japan). The final products were sequenced after cloning into the TOPO TA cloning vector (Invitrogen).

PCR tracing of individual clones

To trace individual clones by amplifying unique genomic-proviral junction, primer pairs located in the genome and vector were used. LTR3 was used as the 5′ primer. The 3′ primer was designed from the genomic-proviral junction sequence after determining its precise location in the human genome by comparison to known genomic sequences using a basic local alignment search tool (BLAST) search (Table S1 on the *Blood* website; see the Supplemental Table link at the top of the online article). For semiquantitative PCR, primers located in GFP cDNA (5′ primer: CCA GTT CAG CGT GTC CGG CG; 3′ primer: GGG GTC TTT GCT CAG GGC GG) were used. AmpliTaq and reagents were purchased from Takara Shuzo (Otsu, Japan). PCR conditions for 100 ng of each sample DNA were set as follows: 30 cycles consisting of denaturation at 94°C for 1 minute, annealing at 60°C for 1 minute, and elongation at 72°C for 2 minutes with a

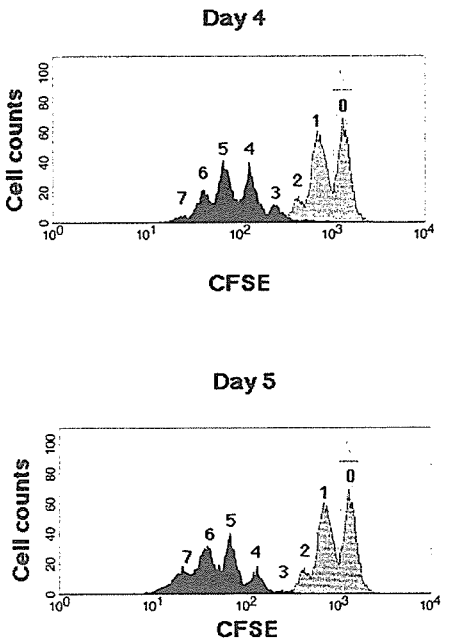

Figure 1. Kinetics of CB CD34⁺ cells during SFSD culture. Representative flow cytometric profiles of CFSE-labeled CB CD34⁺ cells. CB CD34⁺ cells were stained with CFSE and cultured in the SFSD system. The fluorescence intensity was analyzed at 2 days (gray histogram), 4 days (top, black histogram), and 5 days (bottom, black histogram) after culture. The number above each peak represents the number of divisions according to the fluorescence intensity. The relative frequencies of undivided cells were 51.24% ± 3.12% % at day 2, 0.09% ± 0.04% at day 4, and 0.04% ± 0.03% at day 5 (n = 3). The fluorescence intensity of the cells incubated with colcemid confirms the position of the cells that have not divided (dotted line).

2-second extension in each additional cycle, and final reaction at 71°C for 8 minutes followed by gradual cooling to 4°C. Amplified products were loaded on 2% agarose gels.

Statistical analysis

The data from several limiting dilution experiments were combined and used for analysis. The frequency of SRCs in the test BM sample was calculated by applying Poisson statistics to the proportion of negative recipients at different dilutions using L-Calc software (StemCell Technologies, Vancouver, BC, Canada). Data are represented as mean plus or minus standard error (SE). The 2-sided *P* value was determined, testing the null hypothesis that the 2 population medians are equal. *P* values less than .05 were considered to be significant.

Results

Cell division kinetics and SRC expansion during SFSD culture

Cell division kinetics during culture were assessed by a high-resolution procedure for tracking cells using their proliferation history, based on the loss of cellular fluorescence after staining with CFSE (Figure 1). Flow cytometric analysis of CD34⁺ cells harvested from 4- and 5-day cultures resolved more than 3 and 4 generations of progeny, respectively. Undivided cells were not detectable, which suggested the possibility of no dormant cells in this system after 4 days of culture.

A quantitative SRC assay was used to compare the frequency of SRCs between uncultured and cultured CD34⁺ cells in this system. When purified CD34⁺ cells were cultured for 5 days, the total number of cells had expanded 20.1-fold ± 2.7-fold (n = 10). Since 63.6% ± 4.2% (n = 10) of cells were CD34⁺ after culture, CD34⁺ cells had increased around 12.8-fold. A graded number of CD34⁺ cells were transplanted intravenously into irradiated NOD/SCID mice. Human cell engraftment in mice was determined 10 weeks after transplantation (Table 1). The frequencies of SRCs in uncultured and cultured CD34⁺ cells were 1 per 25 794 cells (95% CI; 14 408 to 46 177 cells) and 1 per 34 056 cells (95% CI; 19 072 to 60 810 cells), respectively. Thus, the calculated change in the total SRC numbers following culture was about a 9.8-fold increase. However, the result does not directly demonstrate that each HSC has multiplied 9.8 times through self-renewal divisions in vitro, since the changes of homing and proliferative abilities following culture may also affect results of the SRC assay. Clonal analysis is a more accurate method to demonstrate true SRC multiplication.

Quantitative SRC assay of gene-marked CD34⁺ CB cells before and after SFSD culture

To set up clonal analysis, ex vivo expansion of gene-marked SRC was measured by quantitative SRC assay. CD34⁺ CB cells were infected with recombinant lentivirus containing cDNA encoding for enhanced green fluorescent protein (EGFP), and 42% ± 7% (n = 26) of the CD34⁺ cells subsequently expressed EGFP 4 days after infection. The infection conditions were optimized to minimize the probability of multiple integrations into target cells.[22] This time, the SRC "expansion" was measured by transplanting the graded number of cells before culture and their whole progeny after 4 days of culture (Figure 2A). Both CD19⁺EGFP⁺ lymphoid and CD33⁺EGFP⁺ myeloid reconstitution were detected in each mouse when human CD45⁺EGFP⁺ cells were engrafted (Figure 2B). The calculated frequencies of EGFP⁺ SRCs before and after culture were 1 per 23 304 cells (95% CI; 17 147 to 31 672 cells) and 1 per 4633 cells (95% CI; 3674 to 5842 cells), respectively, making the fold expansion 5.03 (Figure 2C).

In vitro SRC multiplication at clonal level

To detect multiplied clones, 5×10^4 gene-marked CD34⁺ cells were cultured for 4 days and then divided into 10 lots, each of which was transplanted directly into the bone marrow of a NOD/SCID mouse (Figure 3A). While the seeding efficiency of intravenously transplanted human cells into NOD/SCID mice is less than 10%, iBMT negates the effect of homing, allowing efficient detection of amplified SRCs.[18] We used linear amplification-mediated (LAM)–PCR[23] to detect unique genomic-proviral junctions as clonal markers. Detection of the same clones in different mice would provide direct evidence of ex vivo multiplication of an SRC clone. We identified 20 clone-specific genomic-proviral junction sequences by LAM-PCR on 10 mice (Table 2).

Table 1. Comparison of the frequency of SRCs in pre- and postcultured CD34⁺ CB cells by limiting dilution assay

No. CD34⁺ cells transplanted	Engraftment with precultured cells	Engraftment with postcultured cells
100 000	5/5	5/5
50 000	7/9	6/9
10 000	5/10	4/10
5 000	0/5	0/5

The graded number of pre- and postcultured CD34⁺ CB cells were transplanted into irradiated NOD/SCID mice (n = 58) intravenously. At 10 weeks after transplantation, human cell engraftment in mice was determined by flow cytometric analysis. The detection of human cells was also confirmed by PCR of the human chromosome 17–specific α-satellite primers (data not shown). SRC frequencies were calculated using Poisson statistics and the method of maximum likelihood with the assistance of L-Calc software (StemCell Technologies). Engraftment values indicate number of engrafted mice/number of transplantations.

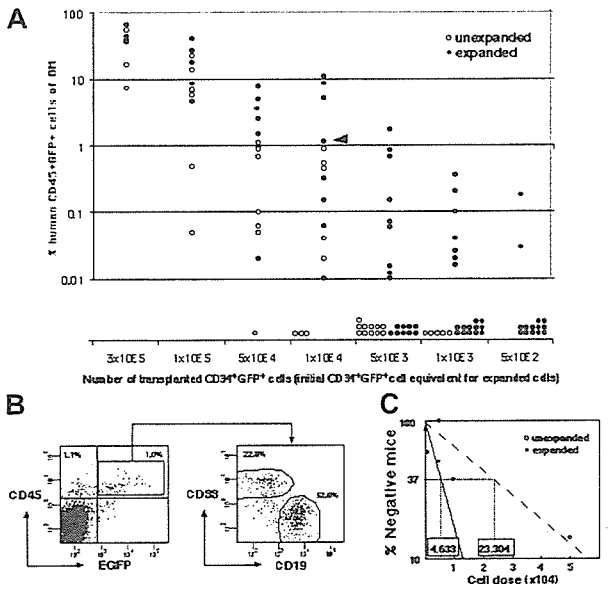

Figure 2. Comparison of the frequency of infected SRCs with and without SFSD culture. (A) The infected cells were divided into 2 groups consisting of the same number of cells (5×10^2, 1×10^3, 5×10^3, 1×10^4, 5×10^4, 1×10^5, 3×10^5 cells/mouse). One group was instantly transplanted (n = 41), and the other was cultured for 4 days in SFSD culture, and then transplanted into NOD/SCID mice (n = 75). At 10 weeks after transplantation, the mice were killed and the percentages of $CD45^+EGFP^+$ cells in the mouse bone marrow cells were determined by flow cytometry. The presence of cells was also confirmed by PCR using EGFP primers to rule out the false-positive results by flow cytometry (data not shown). (B) Representative FACS profiles. Data from mouse, indicated by the triangle in panel A, are shown. The numbers in the top left and right quadrants show the percentage of $CD45^+EGFP^-$ and $CD45^+EGFP^+$ populations, respectively. Multilineage repopulation capacity of transduced SRCs was also examined. The numbers in the right panel show the percentage of $CD33^+$ and $CD19^+$ populations within $CD45^+EGFP^+$ cells from bone marrow. (C) The frequency of infected SRCs before and after culture. The number shown within each box indicates the calculated frequency of SRCs using L-Calc software (StemCell Technologies).

Clone-specific primers were designed and PCR was performed to trace each clone within 10 mice. Since the detection sensitivity of a clone by PCR was assumed to be 0.1% by semiquantitative PCR using primers within the EGFP cDNA, clones comprising more than 10^4 cells would be detected by this method. Representative clones are shown in Figure 3B. Although 14 clones were detected in only 1 mouse (such as clones 1-1, 1-4, and 1-15), 6 clones were detected in more than 2 mice. Clones 1-2, 1-7, and 1-16 were detected in 2 mice (data not shown). Clone 1-3 was detected in 4 mice, clone 1-10 was detected in 5 mice, and clone 1-20 was detected in 6 mice. The data suggested that some of clones divided during culture and participated in hematopoietic reconstitution of 2, 4, 5, or 6 independent mice.

Multilineage differentiation of multiplied SRCs at the clonal level

To detect multilineage differentiation of amplified SRCs, purified $CD19^+EGFP^+$ and $CD33^+EGFP^+$ cells from each mouse were analyzed for each clone (Figure 4A). Although gene-marked cultured cells were transplanted into 10 mice, 4 mice died before analysis. We identified 15 clonal markers from the remaining 6 mice by LAM-PCR (Table 2). Purified $CD19^+EGFP^+$ and $CD33^+EGFP^+$ cells from each mouse were examined for the presence of each clone (Figure 4B-C). Twelve clones were present in only 1 mouse. Eleven were present in both $CD19^+$ and $CD33^+$ cells (such as clone 2-7 and 2-14), whereas 1 clone (clone 2-5) repopulated only $CD19^+$ cells. There were 3 clones present in 2 independent mice. Two of them reconstituted both $CD19^+$ and $CD33^+$ cells (clone 2-6 and 2-15), but 1 clone (clone 2-3) reconstituted only $CD19^+$ cells in mouse no. 2 and both $CD19^+$ and $CD33^+$ cells in mouse no. 4. These results demonstrate the multilineage differentiation ability of the multiplied SRC clones in our system.

Self-renewal divisions of multiplied SRCs at the clonal level

Finally, we designed a secondary transplantation experiment to confirm the self-renewal ability of each clone (Figure 5A). We identified 39 clonal markers from 10 primary and 10 secondary transplanted mice by LAM-PCR, 11 of which were detected in multiple mice (Table 2). Twenty-eight clones were present in a single primary recipient and 16 were detected in a secondary recipient. Eleven clones were detected in multiple primary recipients and 14 of 29 clones were detected in a secondary recipient. Representative clones are shown in Figure 5B. Clones 3-5, 3-22, and 3-24 were present in 3 primary mice but only in 1 secondary mouse with lymphomyeloid differentiation ability. Clone 3-13 was present in 4 primary mice but also only in 1 secondary mouse. Similarly, clones 3-7, 3-29, 3-32, and 3-35 were present in 2 primary mice but in only 1 secondary mouse. Clones 3-23, 3-26, and 3-38 were present in 2 to 4 primary mice and transmitted to 2 secondary mice with maintenance of both self-renewal and multilineage differentiation ability. This result demonstrated that some human HSC clones are able to multiply in vitro.

Discussion

Several protocols for ex vivo expansion of human HSCs demonstrated 2- to 4-fold expansion of SRCs by using quantitative SRC

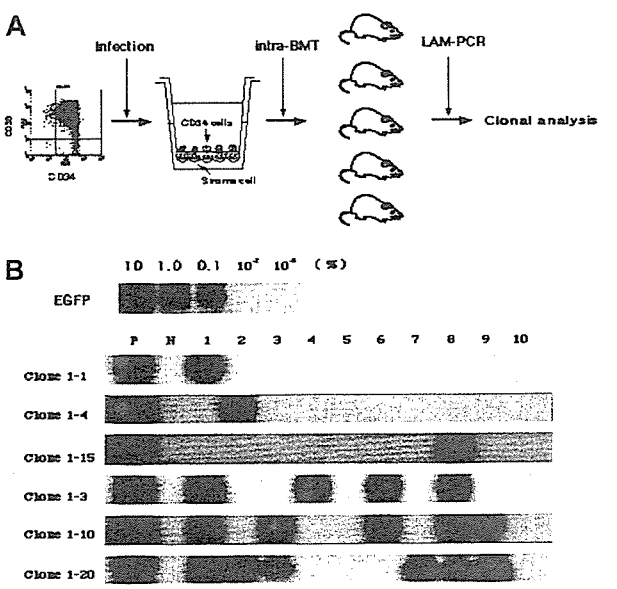

Figure 3. Detection of multiplied SRCs in SFSD culture. (A) Experimental protocol for the detection of multiplied SRCs in SFSD culture. (B) PCR tracing of individual clones in mice that underwent transplantation with SFSD-cultured cells. Representative clones are shown. Each clone was detected by amplifying a unique genomic-proviral junction sequence with primer pairs located in the genome (clone number shown in Table S1) and vector (LTR3). For semiquantitative PCR, genomic DNA from the indicated ratio of mixture of Jurkat cells with and without transduction by recombinant retrovirus MFG-EGFP[22] was used. The numbers at the top indicate each mouse. The numbers on the left indicate each SRC clone. P indicates positive control; N, negative control.

Table 2. Amplification of SRC clones in mice that underwent transplantation with CD34$^+$ cells after SFSD culture

	No. clones (no. mice)	Fold amplification of clones, no. of clones (%)					
		1	2	3	4	5	6
Experiment 1	20 (10)	14 (70)	3 (15)	0 (0)	1 (5)	1 (5)	1 (5)
Experiment 2	15 (6)	12 (80)	3 (20)	0 (0)	0 (0)	0 (0)	0 (0)
Experiment 3	39 (10)	28 (71.8)	6 (15.4)	3 (7.7)	2 (5.1)	0 (0)	0 (0)
Total	74	54	24	9	12	5	6

SFSD-cultured CD34$^+$ cells were divided into 10 groups, and transplanted directly into the bone marrow of 10 mice. In experiment 2, 4 mice died before examination. If the same clone was engrafted in 3 mice, it was assumed that the clone was amplified 3-fold by SFSD culture.

assay.[6-9] However, it does not mean a 2- to 4-fold increase of SRC numbers because it is difficult to distinguish between a truly increased SRC number or increased SRC proliferative potential following culture (and therefore increased human engraftment detection) by this assay.[22] On the other hand, recent data suggest that surface expression of CXCR4 and CD26 in CD34$^+$ cells by ex vivo manipulation have a positive and negative effect, respectively, on their homing and engraftment in NOD/SCID mice.[24,25] Thus, the true self-renewal division of SRCs in vitro could not be assessed by the quantitative SRC assay. By using lentiviral gene-marking and iBMT of cultured CD34$^+$ CB cells, we have successfully dissected the relative contribution of clonal multiplication from homing efficiency and/or proliferative potential on SRC "expansion."

We have previously demonstrated that iBMT is 15 times more sensitive than conventional intravenous injection for the detection of SRCs.[18] In an attempt to improve the efficiency of homing, seeding, and repopulation, iBMT has been applied to detect clones used to repopulate different individuals.[26] If the number of SRCs amplified 5-fold during culture, we should ideally find every clone in 5 different mice when cultured cells are divided and transplanted by this method into 10 mice. However, as shown in Table 2, 74 clones were detected in 110 mice that underwent transplantation. Therefore, the net amplification of SRCs was calculated to be at least 1.5-fold. The discrepancy between 1.5-fold amplification from clonal analysis and 5.03-fold expansion from the quantitative SRC assay may be due to the increased SRC proliferative potential and/or homing and engraftment efficiency following culture, which affects the quantitative SRC assay using intravenous injection.[22,24,25] To further dissect these 2 factors, comparing cultured cells by limiting dilution using iBMT and clonal analysis would be useful. Further study is required to elucidate their relative contribution.

Dividing HSCs in vitro resulted in depletion, maintenance, or expansion (Figure 6). Of 74 clones analyzed in the 3 experiments

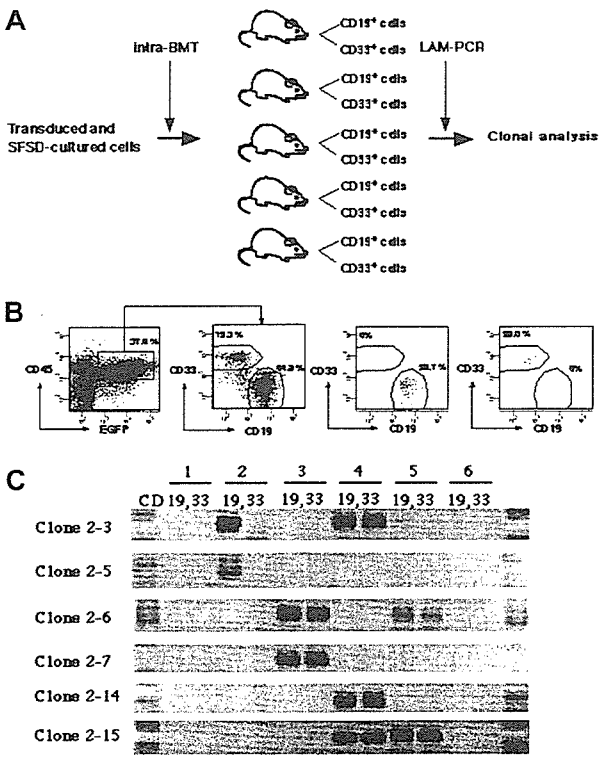

Figure 4. Detection of multilineage differentiation by multiplied SRCs. (A) Experimental protocol for the detection of multilineage differentiation by multiplied SRCs. (B) At 10 weeks after transplantation, the mice were killed and CD33$^+$ and CD19$^+$ populations within CD45$^+$EGFP$^+$ cells from bone marrow were sorted. The numbers in the panels show the percentage of the gated cells. Sorted CD19$^+$EGFP$^+$ and CD33$^+$EGFP$^+$ cells show more than 99% pure fractions. (C) PCR tracing of individual clones in CD19$^+$EGFP$^+$ and CD33$^+$EGFP$^+$ cells from mice that underwent transplantation with SFSD-cultured cells. Each clone was detected by amplifying a unique genomic-proviral junction sequence with primer pairs located in the genome (clone number shown in Table S1) and vector (LTR3). The numbers at the top indicate each mouse. The numbers on the left indicate each SRC clone.

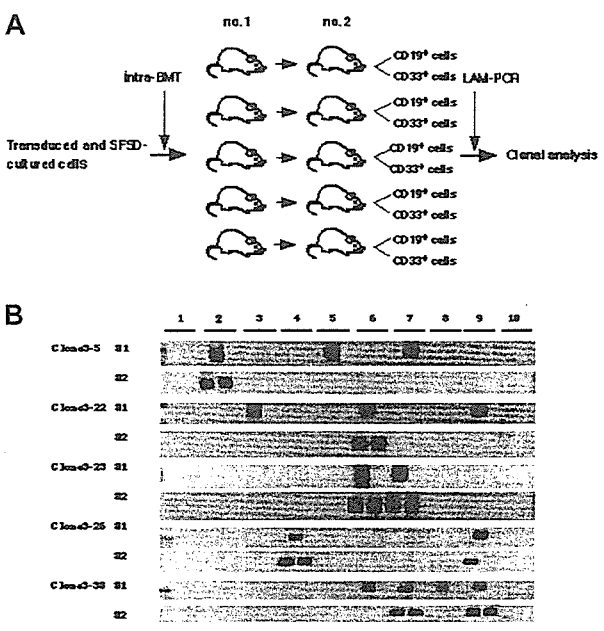

Figure 5. Detection of self-renewal and multi-lineage differentiation by multiplied SRCs. (A) Experimental protocol for the detection of self-renewal and multilineage differentiation by multiplied SRCs. (B) PCR tracings of individual clones in bone marrow cells from mice that underwent transplantation with SFSD-cultured cells are shown in column 1. The bone marrow cells were then transplanted into secondary mice. PCR tracings of individual clones in CD19$^+$EGFP$^+$ and CD33$^+$EGFP$^+$ cells from the secondary mice are shown in column 2. Each clone was detected by amplifying a unique genomic-proviral junction sequence with primer pairs located in the genome (clone number shown in Table S1) and vector (LTR3). The numbers at the top indicate each mouse. The numbers on the left indicate each SRC clone.

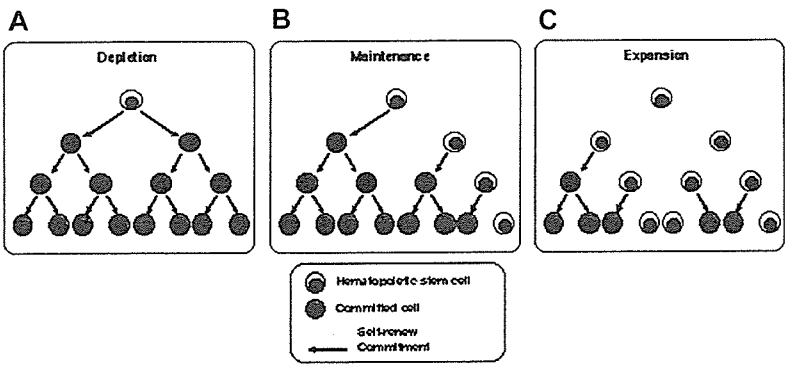

Figure 6. Schematic demonstration of the fate of HSCs in vitro. The fates of HSCs in SFSD culture are shown as depletion (A), maintenance (B), and expansion (C). Our data indicate that 73% of HSCs were maintained and 27% expanded in SFSD culture.

presented here, 54 clones (73%) were present in 1 individual, which means that HSCs were dormant or maintained during culture. Contribution of dormant HSCs to this result is negligible, since more than 99.9% of $CD34^+$ cells proliferated in the SFSD culture system (Figure 1) and the SRC frequency by iBMT was 1 in 44 $CD34^+CD38^-$ cells and 1 in 1010 Lin^-CD34^+ cells.[18,27] Glimm and Eaves[17] also demonstrated that the vast majority of SRCs present in 5-day cultures of CB $CD34^+$ cells stimulated with cytokines had executed at least 3 full cell cycles. Therefore, asymmetric self-renewal division would result in HSC maintenance in this population (Figure 6B). Twenty clones (27%) divided and resulted in multiplication up to 6 times after culture. Furthermore, 3 clones, clones 3-23, 3-26, and 3-38, multiplied and maintained both multilineage differentiation and self-renewal activity. This indicates symmetric self-renewal division of HSCs at some stage during culture (Figure 6C). Therefore, there are at least 2 classes of HSCs, each of which behaves differently in SFSD culture: maintaining HSCs and multiplying HSCs. Identification of the differences between these 2 populations with respect to surface markers, state of gene expression, or other behaviors such as status of interaction with stromal cells in vitro, would greatly facilitate the development of an optimal culture system for ex vivo expansion. Assessment of the biologic function of individual human HSCs would also provide a powerful tool for the characterization of cellular and molecular determinants that govern their reconstitution ability.

New classes of SRCs have been recently identified.[13,28-30] While we focused on long-term repopulating cells (LTRCs) in this study, it is of interest to determine what other types of SRCs also expanded in the SDSF culture system. Rapid-SRCs (R-SRCs) identified in $Lin^-CD34^+CD38^{low}CD36^-$ cells repopulate the myeloid and erythroid lineage within 2 weeks of iBMT.[28] Because we did not analyze at 2 weeks after transplantation and the long-term fate of R-SRCs has not been shown, we could not determine their contribution in this study. Short-term repopulating cells (STRCs) with lymphomyeloid differentiation potential were identified by transplanting $CD34^+CD38^+$ cells into NOD/SCID-β2 microglobulin-null mice.[29] Since we did not examine the presence of STRCs in NOD/SCID mice at 10 weeks after iBMT, we could not exclude the possibility that the 27 clones that did not transmit to secondary hosts in experiment 3 (Table 2) were STRCs. While we believe that most of the clones identified in this study were LTRCs, clonal analysis at an early time point after transplantation is required to determine the magnitude of expansion of STRCs and R-SRCs. Further study would also reveal the extent of clonal exhaustion of LTRCs during expansion culture.

Collectively, our data demonstrate that current ex vivo expansion conditions result in reliable stem cell expansion, and the clonal tracking we have employed is the only reliable method that can be used in the development of clinically appropriate expansion methods.

Acknowledgments

We thank members of the animal facility and the center for regenerative medicine of Tokai University, especially Mayumi Nakagawa and Tomoko Uno, and members of the Tokai Cord Blood Bank for their assistance. We also thank John Dick for critical reading of the manuscript.

References

1. Williams DA. Ex vivo expansion of hematopoietic stem and progenitor cells: robbing Peter to pay Paul? Blood. 1993:81:3169-3172.
2. Moore MA. Umbilical cord blood: an expandable resource. J Clin Invest. 2000:105:855-856.
3. McNiece I. Ex vivo expansion of hematopoietic cells. Exp Hematol. 2004:32:409-410.
4. Greiner DL, Hesselton RA, Shultz LD. SCID mouse models of human stem cell engraftment. Stem Cells. 1998:16:166-177.
5. Larochelle A, Vormoor J, Hanenberg H, et al. Identification of primitive human hematopoietic cells capable of repopulating NOD/SCID mouse bone marrow:implications for gene therapy. Nat Med. 1996:2:1329-337.
6. Bhatia M, Bonnet D, Kapp U, et al. Quantitative analysis reveals expansion of human hematopoietic repopulating cells after short-term ex vivo culture. J Exp Med. 1997:186:619-624.
7. Conneally E, Cashman J, Petzer A, Eaves C. Expansion in vitro of transplantable human cord blood stem cells demonstrated using a quantitative assay of their lympho-myeloid repopulating activity in nonobese diabetic-scid/scid mice. Proc Natl Acad Sci U S A. 1997:94:9836-9840.
8. Ueda T, Tsuji K, Yoshino H, et al. Expansion of human NOD/SCID-repopulating cells by stem cell factor, Flk2/Flt3 ligand, thrombopoietin, IL-6, and soluble IL-6 receptor. J Clin Invest. 2000:105: 1013-1021.
9. Chute JP, Muramoto G, Fung J, Oxford C. Quantitative analysis demonstrates expansion of SCID-repopulating cells and increased engraftment capacity in human cord blood following ex vivo culture with human brain endothelial cells. Stem Cells. 2004:22:202-215.
10. Ailles L, Schmidt M, Santoni de Sio FR, et al. Molecular evidence of lentiviral vector-mediated gene transfer into human self-renewing, multipotent, long-term NOD/SCID repopulating hematopoietic cells. Mol Ther. 2002:6:615-626.
11. Yahata T, Ando K, Miyatake H, et al. Competitive repopulation assay from two cord blood units of $CD34^+$ cells in NOD/SCID/gammac(null) mice. Mol Ther. 2004:10:882-891.
12. Nolta JA, Dao MA, Wells S, Smogorzewska EM, Kohn DB. Transduction of pluripotent human hematopoietic stem cells demonstrated by clonal analysis after engraftment in immune-deficient mice. Proc Natl Acad Sci U S A. 1996:93:2414-2419.
13. Guenechea G, Gan OI, Dorrell C, Dick JE. Distinct classes of human stem cells that differ in proliferative and self-renewal potential. Nat Immunol. 2001:2:75-82.
14. Kawada H, Ando K, Tsuji T, et al. Rapid ex vivo expansion of human umbilical cord hematopoietic progenitors using a novel culture system. Exp Hematol. 1999:27:904-915.

15. Shimakura Y, Kawada H, Ando K, et al. Murine stromal cell line HESS-5 maintains reconstituting ability of ex vivo-generated hematopoietic stem cells from human bone marrow and cytokine-mobilized peripheral blood. Stem Cells. 2000:18: 183-189.
16. Tsuji T, Ogasawara H, Aoki Y, Tsurumaki Y, Kodama H. Characterization of murine stromal cell clones established from bone marrow and spleen. Leukemia. 1996:10:803-812.
17. Glimm H, Eaves CJ. Direct evidence for multiple self-renewal division of human in vivo repopulating hematopoietic cells in short-term culture. Blood. 1999:94:2161-2168.
18. Yahata T, Ando K, Sato T, et al. A highly sensitive strategy for SCID-repopulating cell assay by direct injection of primitive human hematopoietic cells into NOD/SCID mice bone marrow. Blood. 2003:101:2905-2913.
19. Miyoshi H, Blomer U, Takahashi M, Gage FH, Verma IM. Development of a self-inactivating lentivirus vector. J Virol. 1998:72:8150-8157.
20. Oki M, Ando K, Hagihara M, et al. Efficient lentiviral transduction of human cord blood CD34$^+$ cells followed by their expansion and differentiation into dendritic cells. Exp Hematol. 2001:29:1210-1217.
21. Schmidt M, Hoffmann G, Wissler M, et al. Detection and direct genomic sequencing of multiple rare unknown flanking DNA in highly complex samples. Hum Gene Ther. 2001:12:743-749.
22. Mazurier F, Gan OI, McKenzie JL, Doedens M, Dick JE. Lentivector-mediated clonal tracking reveals intrinsic heterogeneity in the human hematopoietic stem cell compartment and culture-induced stem cell impairment. Blood. 2004:103: 545-552.
23. Schmidt M, Zickler P, Hoffmann G, et al. Polyclonal long-term repopulating stem cell clones in a primate model. Blood. 2002:100:2737-2743.
24. Peled A, Petit I, Kollet O, et al. Dependence of human stem cell engraftment and repopulation of NOD/SCID mice on CXCR4. Science. 1999:283: 845-848.
25. Christopherson KW, Hangoc G, Mantel CR, Broxmeyer HE. Modulation of hematopoietic stem cell homing and engraftment by CD26. Science. 2004:305:1000-1003.
26. Lapidot T, Dar A, Kollet O. How do stem cells find their way home? Blood. 2005:106:1901-1910.
27. Kimura T, Wang J, Matsui K, et al. Proliferative and migratory potential of human cord blood-derived CD34 severe combined immunodeficiency repopulating cells that retain secondary reconstituting capacity. Int J Hematol. 2004:79: 328-333.
28. Mazurier F, Doedens M, Gan OI, Dick JE. Rapid myeloerythroid repopulation after intrafemoral transplantation of NOD-SCID mice reveals a new class of human stem cells. Nat Med. 2003:9:959-963.
29. Glimm H, Eisterer W, Lee K, et al. Previously undetected human hematopoietic cell populations with short-term repopulating activity selectively engraft NOD/SCID-beta2 microglobulin-null mice. J Clin Invest. 2001:107:199-206.
30. Hogan CJ, Shpall EJ, Keller G. Differential long-term and multilineage engraftment potential from subfractions of human CD34$^+$ cord blood cells transplanted into NOD/SCID mcie. PNAS. 2002: 99:413-418.

Clonal analysis of thymus-repopulating cells presents direct evidence for self-renewal division of human hematopoietic stem cells

Takashi Yahata, Shizu Yumino, Yin Seng, Hiroko Miyatake, Tomoko Uno, Yukari Muguruma, Mamoru Ito, Hiroyuki Miyoshi, Shunichi Kato, Tomomitsu Hotta, and Kiyoshi Ando

To elucidate the in vivo kinetics of human hematopoietic stem cells (HSCs), $CD34^+CD38^-$ cells were infected with lentivirus vector and transplanted into immunodeficient mice. We analyzed the multilineage differentiation and self-renewal abilities of individual thymus-repopulating clones in primary recipients, and their descending clones in paired secondary recipients, by tracing lentivirus gene integration sites in each lymphomyeloid progeny using a linear amplification-mediated polymerase chain reaction (PCR) strategy. Our clonal analysis revealed that a single human thymus-repopulating cell had the ability to produce lymphoid and myeloid lineage cells in the primary recipient and each secondary recipient, indicating that individual human HSCs expand clonally by self-renewal division. Furthermore, we found that the proportion of HSC clones present in the $CD34^+$ cell population decreased as HSCs replicated during extensive repopulation and also as the differentiation capacity of the HSC clones became limited. This indicates the restriction of the ability of individual HSCs despite the expansion of total HSC population. We also demonstrated that the extensive self-renewal potential was confined in the relatively small proportion of HSC clones. We conclude that our clonal tracking studies clearly demonstrated that heterogeneity in the self-renewal capacity of HSC clones underlies the differences in clonal longevity in the $CD34^+$ stem cell pool. (Blood. 2006;108:2446-2454)

Introduction

Self-renewal and multilineage differentiation are the 2 fundamental abilities that define hematopoietic stem cells (HSCs) and distinguish them from progenitors. Severe combined immunodeficient mouse (SCID)–repopulating cells (SRCs), originally identified by their ability to reconstitute hematopoiesis in nonobese diabetic (NOD)/SCID mice, are thought to represent human HSCs that are useful clinically to repopulate human recipients.[1-3] Unlike murine HSCs that have been purified and analyzed at the single-cell level,[4] viral gene-marking is the only strategy for the in vivo clonal analysis of human HSCs.[5] Using this approach, several studies documented heterogeneity among SRC clones and implied that some clones have the ability to differentiate into B-lymphoid and myeloid lineages and to self-renew.[6-12] A major shortcoming of using the NOD/SCID mouse model is a lack of reproducible human T-lymphocyte repopulation. Consequently, the multilineage differentiation capacity of SRCs in NOD/SCID recipients has been assessed by reconstitution of only B-lymphoid and myeloid lineages. Because a close relationship between B-lymphocyte and macrophage differentiation has been indicated,[13,14] current analyses cannot clearly distinguish true HSCs from lineage-restricted progenitors such as B-lymphocyte/macrophage progenitors. As a result, the multilineage differentiation and self-renewal of HSCs represented by a single SRC are yet to be proven.

Along with other investigators, we demonstrated that phenotypically normal and polyclonal human T lymphocytes were reproducibly repopulated from human cord blood $CD34^+$ cells in the NOD/SCID/common γ chain (cγ)–null (NOG) mouse.[15-17] Having this unique environment that permits human thymopoiesis, the NOG recipient serves as an excellent model to study self-renewal, as well as multilineage differentiation, of human HSCs. HSCs can be identified as thymus-repopulating cells and distinguished from short-lived oligopotent or monopotent progenitors. Thymopoiesis requires constant recruitment of progenitors into the thymus, which eventually produces mature T lymphocytes in a relatively short period of time.[18,19] Therefore, to maintain thymopoiesis in recipient mice, transplanted HSCs must divide without loss of thymus-repopulating activity. Several classes of SRCs that differ in their proliferative and self-renewal potential have been reported.[20-22]

From the Division of Hematopoiesis, Research Center for Regenerative Medicine, Tokai University School of Medicine, Isehara, Kanagawa; the Department of Hematology, Tokai University School of Medicine, Isehara, Kanagawa; the Central Institute for Experimental Animals, Kawasaki, Kanagawa; the BioResource Center, RIKEN Tsukuba Institute, Tsukuba, Ibaraki; and the Department of Cell Transplantation & Regenerative Medicine, Tokai University School of Medicine, Isehara, Kanagawa, Japan.

Submitted February 8, 2006; accepted May 20, 2006. Prepublished online as *Blood* First Edition Paper, June 6, 2006; DOI 10.1182/blood-2006-02-002204.

Supported by a Grant-in-Aid for Research of the Science Frontier Program and a Grant-in-Aid for Scientific Research from the Ministry of Education, Culture, Sports, Science, and Technology of Japan and by a Research Grant on Human Genome, Tissue Engineering (H17-014), from the Japanese Ministry of Health, Labor, and Welfare, Japan.

T.Y. designed and performed the research, analyzed the data, and wrote the paper; S.Y., Y.S., H. Miyatake, and T.U. performed the research; Y.M. analyzed the data and wrote the paper; M.I., H. Miyoshi, and S.K. provided vital reagents; T.H. analyzed the data; K.A. designed the research, analyzed the data, and wrote the paper.

The online version of this article contains a data supplement.

Reprints: Kiyoshi Ando, Department of Hematology, Tokai University School of Medicine Bohseidai, Isehara, Kanagawa 259-1193, Japan; e-mail: andok@keyaki.cc.u-tokai.ac.jp.

The publication costs of this article were defrayed in part by page charge payment. Therefore, and solely to indicate this fact, this article is hereby marked "advertisement" in accordance with 18 U.S.C. section 1734.

Analyzing the thymus-repopulating activity of these cells provides a unique way to distinguish and identify long-term self-renewing stem cells within the SRCs. Self-renewal of HSCs has been assessed by serial transplantation on the basis that HSCs, which are responsible for multilineage hematopoiesis in primary recipients, are also capable of repeating this process in secondary transplant recipients. Confirmation of the persistence of thymus-repopulating cells with multilineage differentiation ability in the secondary recipient would eliminate the possible contribution of some long-lived progenitors and mature cells and at the same time, provide direct evidence for self-renewal of SRCs.

In this study, we established a novel strategy to analyze both self-renewal and multilineage differentiation of a single human thymus-repopulating SRC clone in NOG recipient mice using linear amplification-mediated polymerase chain reaction (LAM-PCR) that verifies individual genomic virus integration sites by direct sequencing.[23] The identification of specific clones in fluorescent-activated cell sorter (FACS)–sorted lymphomyeloid lineage populations by their unique molecular markers allowed us to assess how individual clones contribute to the specific lineages during long-term hematopoiesis in vivo. We focused on CD4/CD8 double-positive (DP) immature thymocyte populations as a starting point of our clonal analysis of the human HSC ability. Our study presented direct clonal evidence that a single human HSC had the ability to produce lymphoid and myeloid lineage cells. Self-renewal division of multilineage clones resulted in expansion of SRCs. However, this clonal expansion of SRCs leads to the clonal exhaustion of SRCs during long-term hematopoiesis in vivo. It was also indicated that, although most of the SRC clones were destined to loose their self-renewal potential, the relatively small proportion of SRC clones retained extensive self-renewal potential.

Materials and methods

Collection and purification of human CB CD34$^+$CD38$^-$ cells

CB samples were obtained from full-term deliveries according to the institutional guidelines approved by the Tokai University Committee on Clinical Investigation. Mononuclear cells (MNCs) were isolated by Ficoll-Hypaque (Lymphoprep, 1.077 ± 0.001 g/mL; Nycomed, Oslo, Norway) density gradient centrifugation. CD34$^+$ cell fractions were prepared using the CD34 Progenitor Cell Isolation Kit (Miltenyi Biotec, Sunnyvale, CA) according to the manufacturer's directions. Column-enriched CD34$^+$ cells were cryopreserved in liquid nitrogen until use. For isolation of CD34$^+$CD38$^-$ cells, pooled CD34$^+$-enriched cells from multiple donors were stained with fluorescein isothiocyanate–conjugated anti-CD34 (581; Coulter/Immunotech, Marseille Cedex, France), and phycoerythrin (PE)–conjugated anti-CD38 (HB7; BD Biosciences, San Jose, CA) monoclonal antibodies (mAbs). Cells were sorted using the FACSVantage flow cytometer (BD Biosciences) equipped with HeNe and argon lasers. CD38$^-$ gate was determined in reference to isotype control. CD34$^+$CD38$^-$ cells, which comprise 5% to 8% of the total CD34$^+$ cell population, were isolated with 97% to 99% (n = 16) purity using FACSVantage (BD Biosciences).

Lentivirus infection

Purified CD34$^+$CD38$^-$ cells were plated on fibronectin CH-296 fragment and incubated with highly concentrated viral supernatant at a multiplicity of infection (MOI) of 50 in serum-free StemPro-34 medium (Invitrogen, Carlsbad, CA) containing cytokines (Takara Shuzo, Tokyo, Japan) for 16 hours. Recombinant human thrombopoietin (50 ng/mL; kindly donated by Kirin Brewery, Tokyo, Japan), stem cell factor (50 ng/mL; donated by Kirin Brewery, Tokyo, Japan), and Flk-2/Flt-3 ligand (50 ng/mL; R&D Systems, Minneapolis, MN) were used. The number of virus integration sites per cell was examined in the following experiment. CD34$^+$ cells were infected with enhanced green fluorescent protein (EGFP) at an MOI of 50 and then plated in methylcellulose. Individual colonies expressing EGFP were picked up and analyzed for integration sites by LAM-PCR. Over the 20 colonies examined, none of the colonies demonstrated multiple bands, confirming that the individual colonies contain a single integration site (data not shown).

Estimation of multilineage differentiation potential of SRCs

NOD/Shi-scid, IL-2Rγc^{null} (NOG) mice were obtained from the Central Institute for Experimental Animals (Kawasaki, Japan) and maintained in the animal facility of the Tokai University School of Medicine in microisolator cages; the animals were fed with autoclaved food and water. Nine- to 20-week-old NOG mice were irradiated with 250 cGy X-rays. The following day, transduced CD34$^+$CD38$^-$ cells (1×10^4 cells) were injected intravenously into the NOG mice. All experiments were approved by the animal care committee of Tokai University. Sixteen to 20 weeks after transplantation, the mice were humanly killed, and bone marrow (BM) cells, splenocytes, and thymocytes were analyzed by flow cytometry. Cells were stained with mAbs to human leukocyte differentiation antigens. Human hematopoietic cells were distinguished from mouse cells by the expression of human CD45. APC-conjugated anti–human CD19 mAb (Coulter/Immunotech), ECD-conjugated anti–human CD8 and CD34 mAbs (all Coulter/Immunotech), and PE-conjugated anti–human CD3, CD4, and CD33 mAbs were used. The efficiency of gene transduction was determined by the percentage of cells expressing EGFP. EGFP-expressing CD45$^+$ human hematopoietic cells were further classified into human stem/progenitor (CD34$^+$), myeloid (CD33$^+$), B-lymphoid (CD19$^+$), and T-lymphoid (CD3$^+$ or CD4$^+$/CD8$^+$) subpopulations and were sorted using a FACSvantage Diva option (BD Biosciences). To eliminate the contamination of lineage-committed cells, CD34$^+$ cells were sorted on CD19$^-$ and CD33$^-$ gate. Sorted cells, confirmed to be lineage$^{-/low}$CD34$^+$, were designated as stem/progenitor cells. Double cell-sorting was performed to ensure greater than 99% cell purity. Representative FACS profiles of sorting purity were demonstrated in Figure S1 (available at the *Blood* website; see the Supplemental Materials link at the top of the online article).

Secondary transplantation

BM cells were obtained from mice that received a transplant with CD34$^+$CD38$^-$ cells at 13 to 19 weeks after transplantation. The BM cells of these primary recipients were divided equally and injected intravenously into 2 sublethally irradiated secondary NOG recipients (1.35×10^7–2.1×10^7 cells per recipient). Thirteen to 19 weeks after transplantation, BM cells and thymus were collected from each secondary recipient and used for flow cytometric analysis and lineage cell sorting as described.

Integration site analysis of lentivirally marked SRCs

LAM-PCR was carried out as described previously[24] with some slight modifications. Genomic DNA samples (100 ng), isolated from each sorted subpopulation, were preamplified for a total of 100 cycles by repeated primer extension using 0.25 pmol vector-specific, 5′-biotinylated primer LTR1 (5′-GAACCCACTGCTTAAGCCTCA-3′) using ProofStart DNA polymerase (2.5U; Qiagen, Hilden, Germany). The biotinylated extension products were collected using streptavidin-conjugated magnetic beads (Dynal, Oslo, Norway), and the second strand was synthesized using Klenow polymerase (2 U; Takara Shuzo) and random primer (Takara Shuzo). To prevent virus-vector sequence contamination, samples were first incubated with SacI endonuclease (5 U; Promega, Madison, WI) for 2 hours at 37°C and then digested with Tsp509I endonuclease (5 U; New England BioLabs, Ipswich, MA) for 2 hours at 65°C. After restriction digestion, 100 pmol of a linker cassette (5′-GTACATATTGTCGTTAGAACGCGTAAT-ACGACTCACTATAGGGAGA-3′) was ligated using a DNA ligation kit (Takara Shuzo) at 16°C overnight. Each ligated sample was amplified using a vector-specific primer, LTR2 (5′-AGCTTGCCTTGAGTGCTTCA-3′),

and a linker cassette primer (5′-GTACATATTGTCGTTAGAACGCGTA-ATACGACTCA-3′), using the following conditions: 95°C for 1 minute, 60°C for 1 minute, 72°C for 1 minute (30 cycles). Each PCR product was subjected to nested PCR with the internal primers, LTR3 (5′-AGTAGTGTGTGCCCGTCTGT-3′) and LC2 (5′-CGTTAGAACGCGTA-ATACGACTCACTATAGGGAGA-3′), under identical conditions. PCR products were sequenced after cloning into the TOPO TA cloning vector (Invitrogen). The proviral integration sites of DP cells were sequenced, and the sequences were examined for alignment to the human genome using NCBI BlastN (http://www.ncbi.nlm.nih.gov/blast). The verified genomic sequence information of these DP cell integration sites was used to design new primers (all primer sequences used in this study are listed in Tables S1-S3). PCR was performed on each LAM-PCR product using the unique genomic flanking primers in combination with the LTR3 primers.

Estimation of clone size by real-time quantitative PCR (RQ-PCR)

Genomic DNA samples from CD34$^+$ cells of secondary recipients were amplified using multiple displacement amplification reagents (REPLI-g; Qiagen) according to the manufacturer's instructions.[25] Briefly, 10 ng template DNA was mixed with the DNA polymerase and incubated for 16 hours at 30°C. Approximately 50 μg amplified DNA was obtained from each sample. For RQ-PCR, each target DNA was amplified on the same plate with β-globin as the reference using the QuantiTect SYBR Green PCR Master Mix (Qiagen) and the ABI Prism 7700 Sequence Detection System (Applied Biosystems). The relative clone amounts and range were determined in reference to β-globin. Threshold cycles (C_T) were determined as to fit all samples in logarithmic phase. To ensure the efficiency of amplification and the assay precision, calibration curves for each clone sequence were constructed to have the correlations (r^2) of above 0.95 and the efficiency of greater than 98%. A comparative C_T was used to determine the proportion of CD34$^+$ clones in paired secondary recipients that were derived from the parent primary recipient clone. For each sample, the clone C_T value was normalized using the formula $\Delta C_T = \Delta C_T$ clone $- \Delta C_T$ β-globin. To determine relative clone size, the following formula was used: $\Delta\Delta C_T = \Delta C_T$ clone in CD34+ cells of the one secondary recipient $- \Delta C_T$ clone in CD34+ cells of the other secondary recipient, and the value was calculated by the expression $2^{-\Delta\Delta CT}$. Each reaction was performed at least in triplicate. Amplification conditions were as follows: 95°C for 15 minutes followed by 40 cycles at 95°C for 15 seconds, 60°C for 30 seconds, and 72°C for 60 seconds.

The same primer set described in PCR tracking of LAM-PCR procedure was used to amplify each clone. As an internal control, human hematopoietic cell kinase 1 (*HCK1*) gene and ribosomal DNA (*rDNA*) gene were also amplified. Even amplification of each genomic DNA was confirmed by RQ-PCR using all 3 internal control primers (data not shown).[26] The primers for β-globin gene were forward, 5′-GTGCACCTGACTCCTGAG-GAGA-3′, and reverse, 5′-CCTTGATACCAACCTGCCCAG-3′. Primers for *HCK1* gene were forward, 5′-TATTAGCACCATCCATAGGAGGCTT-3′, and reverse, 5′-GTTAGGGAAAGTGGAGCGGAAG-3′. Primers for *rDNA* gene were forward, 5′-CCATCGAACGTCTGCCCTA-3′, and reverse, 5′-TCACCCGTCGTCACCATG-3′.

Statistical analysis

Data are represented as mean ± SD. The 2-sided P value was determined by testing the null hypothesis that the 2 population medians are equal. P values less than .05 were considered to be significant.

Results

Multilineage differentiation of gene-marked SRCs

To investigate the multilineage differentiation and self-renewal capacity of individual SRC clones, we introduced recombinant lentiviral vector carrying an EGFP-encoding gene to cord blood CD34$^+$CD38$^-$ cells which can provide long-term engraftment (more than 12 weeks) and multilineage differentiation,[2] and then we transplanted these cells into sublethally irradiated NOG mice. Multilineage differentiation was determined as the proportion of each hematopoietic lineage within the EGFP-expressing human CD45$^+$ cell population using FACS at 16 to 20 weeks after transplantation (Figure 1). Consistent with our previous results,[16] substantial engraftment, including CD34$^+$ primitive cells, CD33$^+$ myeloid, CD19$^+$ B-lymphoid, CD3$^+$ mature, and DP immature T-lymphoid cells, was observed in the BM, spleen, and thymus of the NOG mice (Table 1). Because the proportion of nontransduced EGFP$^-$ cells within the human graft and the percentage of EGFP$^+$ cells within each lineage were not significantly different (data not shown), these data indicated that EGFP transduction did not affect the differentiation and proliferation capacity of the SRCs.

Multilineage differentiation of individual thymus-repopulating SRC clones

To analyze the multilineage differentiation capacity of individually transduced SRCs, we performed in vivo integration site analysis by LAM-PCR that can distinguish the progeny of each transduced cell

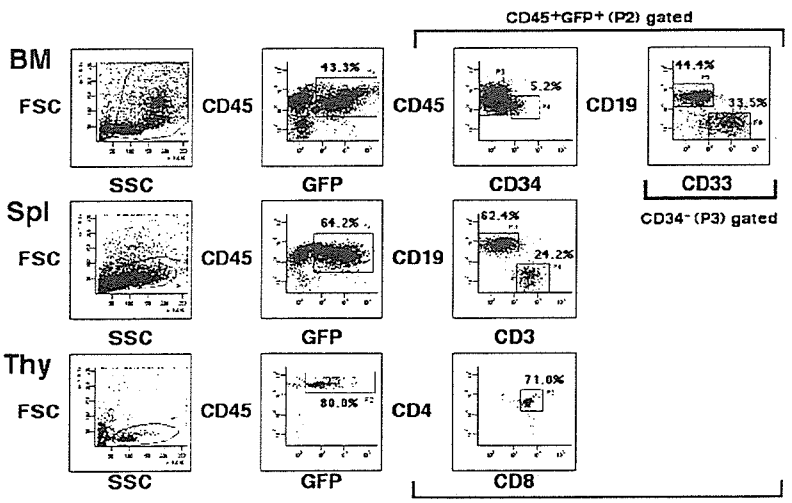

Figure 1. Representative FACS profiles of EGFP-transduced SRCs. Samples were obtained from BM, spleen, and thymus of a NOG mouse, and the proportion of EGFP-transduced human cells was evaluated. The relative frequencies of each cell population are indicated.

Table 1. Proportion of each human cell lineage engrafted in primary NOG mice

Mouse	Week*	Bone marrow, % engrafted					Spleen, % engrafted				Thymus, % engrafted		
		CD45	EGFP	S	M	B	CD45	EGFP	T	B	CD45	EGFP	T
1	17	82.2	84.8	22.1	4.6	ND	81.8	65.3	2.1	88.6	97.8	83.0	82.6
3	17	74.0	58.5	5.2	33.5	44.4	82.1	78.2	24.2	62.4	85.5	80.0	71.0
4	16	88.9	75.4	8.5	17.5	64.4	75.6	77.9	1.6	87.9	95.0	52.9	23.4

The total cellularity of BM and thymus in the primary recipient was $3.56 \times 10^7 \pm 0.53 \times 10^7$ and $1.39 \times 10^5 \pm 1.13 \times 10^5$, respectively. Each mouse listed in the table received a transplant of 10×10^3 $CD34^+CD38^-$ cells.

S indicates $CD34^+$ stem/progenitor cells; M, $CD33^+$ myeloid lineage cells; B, $CD19^+$ B-lymphoid lineage cells; T, $CD3^+$ (spleen) or CD4/CD8 double-positive (thymus) T-lymphoid lineage cells; ND, not done.

*Weeks after transplantation. Bone marrow cells, spleen cells, and thymocytes of NOG mice were stained with an anti–human CD45 mAb and analyzed. The proportion of EGFP-expressing cells within the $CD45^+$ cells and cells positive for each lineage marker in the $CD45^+$/$EGFP^+$ was calculated.

by its unique proviral-genomic fusion sequence (Figure 2A). Direct sequencing of PCR products derived from $EGFP^+CD45^+$ DP cells verified that each product with a unique band length represented individual and different clones. LAM-PCR analysis of $EGFP^+CD45^+$ FACS-purified lineage populations detected multiple integration sites in each cell lineage (Figure 2B). It is reported that the number of vector copies per cell can be controlled by adjusting the MOI, without reducing the transgene expression levels.[27] Because we optimized the experimental conditions to have each cell carrying one insertion per cell, confirmed by both colony-forming assay (see "Materials and methods") and transplantation assay,[24] multiple integration sites detected by LAM-PCR indicated polyclonal repopulation in the NOG mice.

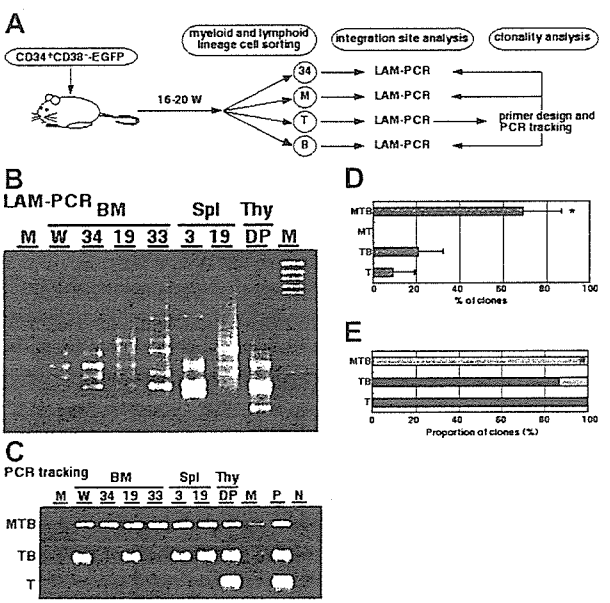

Figure 2. Clonal analysis of primary transplanted SRCs. (A) Study design for clonal analysis of primary grafts. 34 indicates $CD34^+$ stem/progenitor cells; M, $CD33^+$ myeloid lineage cells; B, $CD19^+$ B-lymphoid lineage cells; T, $CD3^+$ (spleen) or CD4/CD8 double-positive (thymus) T-lymphoid lineage cells. (B) Representative LAM-PCR profiles of SRCs. Each band represents a different insertion locus in the assayed material. W indicates unseparated whole BM MNCs; M, size marker. (C) DP-derived T-lymphoid insertion sites were traced by PCR. The clones detected in all lymphomyeloid lineage cells were designated as multipotent type (MTB). TB indicates clones restricted in T-lymphoid and B-lymphoid cells; T, clones detected in T-lymphoid cells; W, unseparated whole BM MNCs; M, size marker; P, TA-cloned LAM-PCR product was used as a positive control; N, DW. (D) Relative frequencies of each clone type detected in primary SRCs. Data represent mean ± SD of 3 independent experiments. $^*P < .01$ relative to other type of clones. (E) The proportion of clones detected in the $CD34^+$ cell population. A total of 27 clones in 3 independent experiments were analyzed. Gray bars represent the clones detected in $CD34^+$ cells. Black bars represent the clones not detected in $CD34^+$ cells. $^*P < .01$ relative to other type of clones.

A total of 27 clones were identified in 3 independent experiments based on the genomic sequence information of the LAM-PCR products from the DP cells (Table S1 summarizes the results of the integration site analysis of DP cells). Using primers designed to correspond to individual integration sites, and therefore unique clones, we were able to track the individual clones and their progenies, including $CD34^+$ stem/progenitor, myeloid, and B-lymphoid cells (Figure 2A). Three different clone types were observed in this experiment (Figure 2C): a multipotent type (MTB), in which insertion sites originally detected in the DP cells were also detected in the highly purified myeloid and B-lymphoid cell populations; a unipotent progenitor containing exclusively T cells; and a bipotent T/B progenitor. However, a bipotent progenitor containing myeloid and T lymphocytes was not detected. As expected, analysis of thymus-repopulating cells revealed that the majority of SRC clones (70.4%) found in the recipient mice were of the MTB multilineage type (Figure 2D; Table 2). We also used CD14 and CD66b, a more mature myeloid marker, for clonal analysis and detected the equivalent proportion of the 3 clone types (data not shown). Interestingly, all MTB clones were found in the $CD34^+$ cell population (Figure 2E), suggesting that the transduced SRC clones self-replicated within the $CD34^+$ stem cell pool without losing their ability to contribute to both lymphoid and myeloid lineages during long-term hematopoiesis. However, as the differentiation capacity of clones became limited to bipotency or unipotency, the proportion of clones that were also found in the $CD34^+$ cell population decreased (Figure 2E), indicating that some SRC clones had been exhausted from the stem cell pool during lineage commitment.

In vivo expansion of individual thymus-repopulating SRC clones

To directly demonstrate the self-renewal capacity of the SRCs, we injected BM cells from each primary mouse into 2 secondary mice

Table 2. Differentiation potential of thymus-repopulating SRC clones

Mouse	No. of clones	Clone type, no. (%)		
		MTB	TB	T
1	5	3 (60)	1 (20)	1 (20)
3	12	7 (58.3)	4 (33.3)	1 (8.3)
4	10	9 (90)	1 (10)	0 (0)
Total	27	19 (70.4)	6 (22.2)	2 (7.4)

Lineage contribution of individual thymus-repopulating SRC clones was evaluated by PCR tracking based on integration site analysis of DP cells. No clones were differentiated into M and T lineages.

MTB indicates clones that gave rise to myeloid (M), T-lymphoid (T), and B-lymphoid (B) lineages; TB, clones differentiated into T and B lineages; T, clones differentiated into T lineage only.

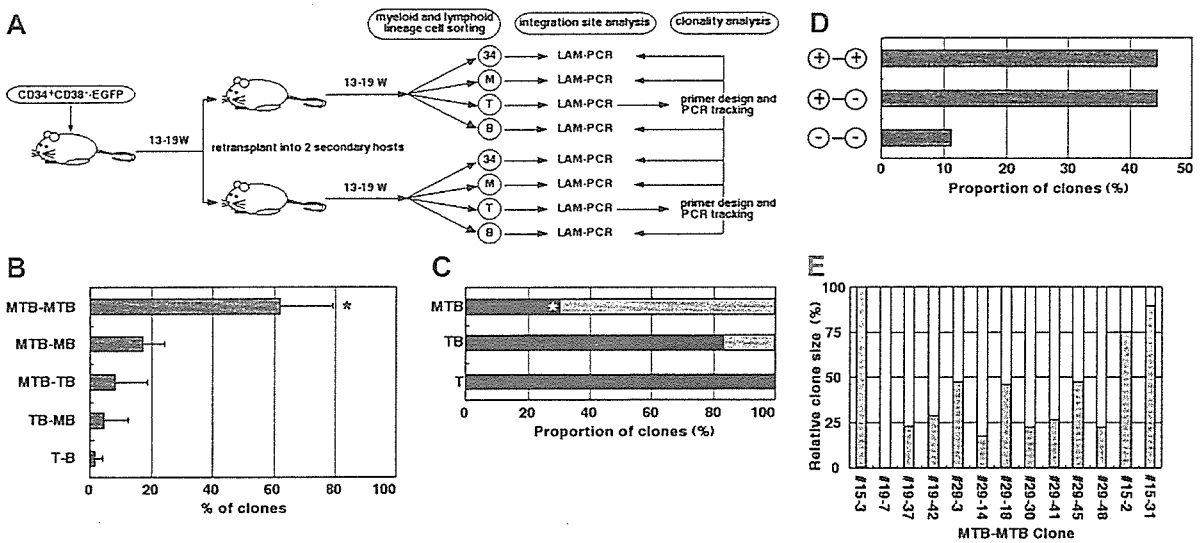

Figure 3. Clonal analysis of secondary transplanted SRCs. (A) Study design for clonal analysis of secondary grafts. 34 indicates $CD34^+$ stem/progenitor cells; M, $CD33^+$ myeloid lineage cells; B, $CD19^+$ B-lymphoid lineage cells; T, $CD3^+$ (spleen) or CD4/CD8 double-positive (thymus) T-lymphoid lineage cells. (B) Relative frequencies of each clone type detected in paired secondary transplanted recipients. Data represent mean ± SD of 3 independent experiments. $^*P < .01$ relative to other type of clones. (C) The proportion of clones detected in $CD34^+$ cells is shown. A total of 43 clones in 3 independent experiments were analyzed. Gray bars represent the clones detected in $CD34^+$ cells. Black bars represent the clones not detected in $CD34^+$ cells. $^*P < .01$ relative to MTB clones found in primary recipients (shown in Figure 1E). (D) The proportion of MTB clones found in $CD34^+$ cells of paired secondary recipients. A total of 27 clones in 3 independent experiments were analyzed. Notation of the left vertical axis: +/+, MTB-MTB clone pairs were detected in $CD34^+$ cells of both secondary recipient pairs; +/−, MTB-MTB clone pairs were detected in the $CD34^+$ cells of 1 of the 2 secondary recipient pairs; and −/−, MTB-MTB clone pairs were not detected in the $CD34^+$ cells of either secondary recipient pairs. (E) Relative clone size of individual clones in each MTB-MTB clone pairs in $CD34^+$ stem cell pool found in paired secondary recipient. The relative clone size of individual clones in 11 MTB-MTB clone pairs detected in $CD34^+$ cells of both secondary recipients was examined by RQ-PCR. The relative clone size of individual clones in each MTB-MTB pair is expressed as the proportion of one clone relative to the other clone. The MTB-MTB clone pairs no.15-3 and no. 19-7 that was detected in the $CD34^+$ cells of only 1 of the 2 secondary recipient pairs were used as experimental control and demonstrated complete skewing to either one recipient.

(Figure 3A). Although each primary BM cell population was divided into 2 recipients, substantial engraftment was observed in these secondary-recipient NOG mice (Table 3). Clone tracking analysis was then performed to examine the fate of individual SRC clones in paired secondary mice. Integration site analysis by LAM-PCR of FACS-sorted cells showed polyclonal reconstitution in each secondary host. A total of 43 clones were identified by integration site analysis of DP T lymphocytes found in 3 secondary recipient pairs (results are summarized in Table S2). All clones detected in paired secondary recipients were also detected in the primary donor. Strikingly, all 43 clones were found as a pair; clones detected in one of the secondary recipient pairs were always observed in the other pair. In greater than 90% of these clone pairs (39 of 43), at least 1 of the daughter clones inherited MTB differentiation potential from its parent clone. Moreover, in 69.2% of these 39 clone pairs, both daughter clones remained multipotent (MTB-MTB type), whereas the other daughter clone in the remaining 30.8% of clone pairs became committed to specific cell lineages (MTB-MB or MTB-TB type) (Figure 3B; Table 4). The existence of MTB-MTB type clones in secondary recipients indicated that a single SRC clone self-replicated in the primary recipients and produced 2 daughter clones that retained SRC potential, thereby resulting in the in vivo expansion of multipotent SRC clones.

Table 3. Proportion of the primary and the secondary human graft

Mouse	Cell dose*	Week†	Bone marrow, %					Thymus, %		
			CD45	EGFP	S	M	B	CD45	EGFP	T
Primary recipient										
101	17	13	80.3	72.7	ND	ND	ND	ND	ND	ND
109	6	19	66.2	71.0	ND	ND	ND	ND	ND	ND
113	10	14	43.2	71.8	ND	ND	ND	ND	ND	ND
Secondary recipient										
101-1	21	13	63.0	93.3	3.4	7.4	63.7	98.2	80.1	83.6
101-2	21	13	62.5	88.1	4.2	14.6	54.9	96.5	78.6	71.2
109-1	13.5	17	29.4	69.4	1.3	49.5	29.9	91.3	78.2	90.5
109-2	13.5	17	33.3	75.1	1.9	27.6	45.9	93.0	70.1	81.1
113-1	19.3	19	72.3	68.7	3.4	17.3	38.7	95.5	88.1	88.0
113-2	19.3	19	86.3	50.0	0.6	17.2	17.3	92.9	72.3	70.3

The total cellularity of BM in the primary and the secondary recipient was $3.86 \times 10^7 \pm 0.83 \times 10^7$ and $3.72 \times 10^7 \pm 0.91 \times 10^7$, respectively. The total cellularity of thymus in the primary and the secondary recipient was $3.36 \times 10^5 \pm 3.28 \times 10^5$ and $2.43 \times 10^5 \pm 1.59 \times 10^5$, respectively.

ND indicates not done.

*Number of $CD34^+CD38^-$ cells transplanted (primary recipient, $\times 10^3$; secondary recipient, $\times 10^6$).

†Number of weeks after transplantation.